Investigation of the Interactions between LOV Domains by Spectroscopic Techniques

By

William H. Newhart

Submitted to the graduate degree program in Chemistry and the Graduate Faculty of the University of Kansas in partial fulfillment of the requirements for the degree of Masters

_____

Chairperson Carey K. Johnson

_____

Cindy L. Berrie

_____

Richard S. Givens

Date Defended: August 25, 2017

The Thesis Committee for William H. Newhart

certifies that this is the approved version of the following thesis:

Investigation of the Interactions between LOV Domains by Spectroscopic Techniques

_____

Chairperson Carey K. Johnson

Date approved: August 25, 2017

Abstract

Plants have adapted a variety of methods necessary for their survival such as stomatal opening and closing, plant growth, and photosynthesis. In order to regulate these processes, plants rely on sensing sunlight in their environment. The plant protein phototropin (PHOT) helps to sense sunlight and transmit the signal downstream to other regulatory proteins.[1] To accomplish light sensing, PHOT contains a pair of blue light sensitive structures referred to as Light, Oxygen, or Voltage (LOV) domains, referred to as LOV1 and LOV2, which interact to regulate downstream cell signaling events. While the photomechanism of how LOV domains sense sunlight has been studied and characterized, the process of how the domains propagate the sensory signal is not well understood.[2, 3]

In this work, spectroscopic methods were employed to investigate the interaction of LOV domains in the dark and when exposed to blue light. Specifically, single molecule burst measurements and stopped-flow spectroscopy were used to detect Förster Resonance Energy Transfer (FRET) between the LOV domains in sample mixtures.

First, single molecule burst measurements were used to probe monomer and dimer formation in samples of labeled LOV from the bacteria *Rhodobacter sphaeroides* (*Rsp*), followed by the attempt to determine the equilibrium dissociation constant (K_d) for *Rsp* LOV. Similar methods were then used to probe the interactions of LOV1 from PHOT of the alga *Chlamydomonas reinhardtii* (*C.r.*). The experimental methods by which we probed the LOV-LOV interactions are presented. A maximum entropy algorithm was used to generate FRET probability distributions from fluorescence measurements on LOV that was placed in the dark (dark-incubated), then exposed to blue light (light-exposed), and then incubated in the dark again

(dark-reverted). To attempt to determine a dissociation constant (K_d), we measured the fluorescence for Rsp mixtures of varying concentration and analyzed the ratios of donor and acceptor channel photons detected to search for a change in the ratio when the concentration of the sample mixture was above or below equilibrium.

LOV from *Rsp* was shown to increase FRET upon dark-reverted incubation of the proteins. The change in FRET may be affected by the concentration of the sample mixture after blue light exposure, the time the sample mixture spent waiting in the dark, and the amount of blue light exposure. In an attempt to determine K_d, we observed FRET between dark-reverted samples that was not accounted for by cross talk and direct excitation of the acceptor, but the data were not conclusive enough to determine a dissociation constant. For *Chlamydomonas reinhardtii* sample mixtures, we observed no noticeable change in the FRET efficiency between dark and light states of *C.r.* LOV1, possibly caused by having one of the two labeled LOV samples in the mixture be photoactive.

Second, we investigated the interaction of *C.r.* LOV1 using stopped-flow spectroscopy to detect FRET between LOV dimers and gain understanding of the kinetics of the interactions. Plots of the data showed a change in the acceptor channel response of labeled *C.r.* LOV1 proteins after exposed to blue light. Based on the recovered time constants from two-component fits of the detector response curves, dimer formation between *C.r.* LOV1 has a fast (~10^1 s) and slow (~10^2-10^3 s) process we attribute to the formation of heterodimers within the mixing chamber and formation of light adapted homodimers prior to mixing.

Acknowledgments

I want to extend my thanks to members of my master's defense committee, Prof. Carey Johnson, Prof. Cindy Berrie, and Prof. Rich Givens for all their advice and help in creating this thesis. I wish to give particular thanks to Prof. Bernhard Dick and Dr. Kathrin Magerl at the University of Regensburg for synthesizing the majority of LOV domains used, their skills and expertise in handling the LOV domains, and their knowledgeable input during Skype meetings and campus visits. I extend a thank you to former Carey Johnson group member Prof. Matthew DeVore, currently at Evangel University, for his overall knowledge, and programming of the maximum entropy algorithm and teaching me how to collect, analyze, and troubleshoot single molecule burst data.

In addition, the Protein Production Group, part of the Center of Biomedical Research Excellence (COBRE) at the University of Kansas, provided mutant variants of LOV from *Chlamydomonas reinhardtii*. I want to thank the production group headed by Dr. Fei Philip Gao and particularly research assistant Anne Cooper for synthesizing the constructs and advising on how to store them. Dr. Nadya Galeva analyzed (by mass spectrometry) nearly all our samples for labeled protein. Mass spectrometry lab director, Dr. Todd Williams, helped to troubleshoot and his advice was always welcome. Undergraduate Ashley McDade assisted with some of our first successful LOV labelings and stop flow measurements, while undergraduate Adebayo Braimah assisted in collecting burst measurements for attempting to determine an equilibrium constant for *Rsp* LOV.

I want to thank Prof. Givens for allowing me to use his laboratory and fluorimeter and Prof. Chris Fischer for allowing use of his stopped-flow instrument. In particular, Prof. Fischer's

former student, Dr. Allen Eastlund, was very helpful, and I thank him for his advice and instruction on how to take stopped-flow measurements. Tom Field, a graduate student in Prof. Michael Johnson's group, was also kind enough to let me use their purified water supply for preparation of buffer solutions. I want also to thank the National Science Foundation for funding.

Finally, and more personally, I wish to thank current and former members of the Carey Johnson group for their time and patience with me over the years. Particularly, I wish to thank my advisor Carey, for his patience and positive outlook in all professional situations. To current members Jacob Johannsen and Sheila Bailey, thank you for the thoughtful discussions and humor. Last but not least, I want to extend special thanks to former colleagues Drs. Eric Rentchler and Andrew Beaven. To Eric, thank you for all the funny jokes and observations. They were most helpful in my times of struggle and I still cherish them. To Andrew, thank you for countless hours of thoughtful conversation, personal advice, and encouragement, whether it was on campus or on the softball field.

Table of Contents

List of Figures

List of Tables

Chapter 1- Background

1.1) Light, Oxygen, or Voltage (LOV) Domains

For plants, being able to sense and react to their environment is crucial for survival. Arguably, there is no more vital resource for plants to detect and utilize than sunlight. Besides being vital for photosynthesis in plants, sunlight also aids in regulating plant processes such as chloroplast aggregation, stomatal opening and closing, and phototropism.[4, 5] Given the diverse functions by which plants rely on sunlight, regulation of such processes is paramount. Phototropin plant proteins are responsible for detecting and propagating the signal of incoming sunlight.[1] This serine/threonine kinase activates auto-phosphorylation whenever exposed to sunlight, specifically blue visible light (~450 nm).[1]

To sense the incoming blue light, phototropins contain a photosensitive polypeptide domain within the N-terminal region of their structure. This polypeptide, a member of the PER/ARNT/SIM (PAS) protein superfamily, is referred to as the LOV domain, due to this family of proteins being able to sense peripheral stimulation such as light, oxygen, or voltage changes.[6] In phototropins, the LOV domain is a ~110 amino acid protein that contains the chromophore flavin mononucleotide (FMN) within its binding pocket, held in place by hydrogen bonding and van der Waals interactions.[1] Upon exposure to sunlight, ~450 nm, an adduct state forms where a covalent bond is created between a cysteine residue embedded within the peptide and the C(4a) carbon of the cofactor's isoalloxazine ring (figure 1.1.1).[7] For phototropins, this excited (adduct) state is impermanent, with the reversion back to the dark state completed within tens or hundreds of seconds for phototropin LOV.[1, 8, 9]

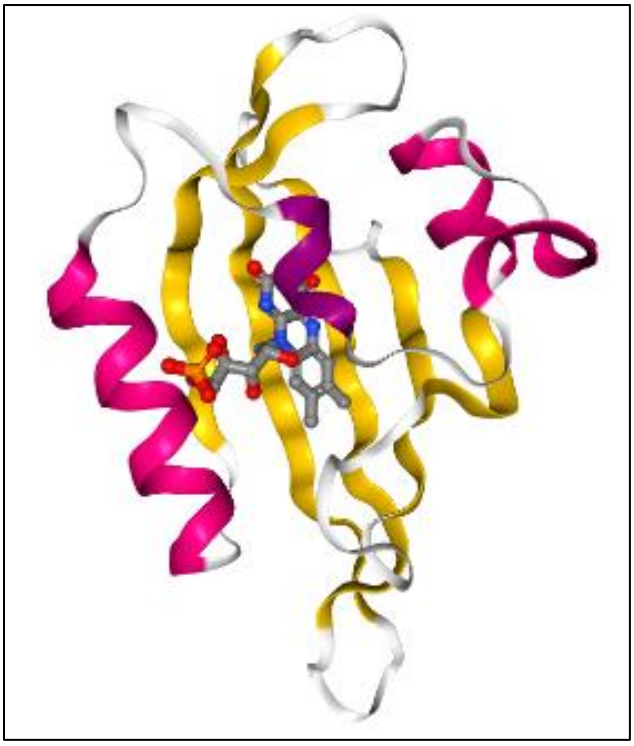

Figure 1.1.1- Dark state crystal structure of a phototropin LOV1 domain from the alga Chlamydomonas reinhardtii (rcsb.org, pdb: 1N9L)

Phototropin contains two LOV domains designated by location relative to the N-terminus of the whole protein (figure 1.1.1).[4] Near the C-terminal end of the protein lies a serine/threonine kinase domain, which is responsible for the autophosphorylation and propagation of the signaling event to other cell structures. Upstream of the kinase exists the Jα helix region, which is bound to LOV2 in the dark state. While the photosensory mechanism of LOV with sunlight has been established, there is still uncertainty as to how phototropin links the photosensory mechanism to the structural and dynamic changes of the kinase needed for signal propagation. It has been hypothesized that structural changes in the Jα helix are in part responsible for regulating the signal between LOV2 and the kinase domain, with LOV2 acting as the primary regulator of kinase activation.[10-13] LOV1 is thought to play a diminished role as a regulator of how sensitive the signaling mechanism is to sunlight.[14]

Regardless of their function, LOV-LOV interactions are vital to cell signal transmission. LOV domains are observed to form dimers and such dimerization is needed for proper cell signaling events to be executed.[14] Published evidence has suggested that LOV domains from different species form stable dimers, and the stability of the dimers may change in the light adduct state.[4, 15-17] Multiple models describing the role of LOV domain dimerization relative to cell signal transmission may be proposed. One potential mechanism involves LOV1 and LOV2 of a single phototropin interacting more strongly with the kinase domain in the dark state. Upon exposure to blue light, the interaction between LOV1-LOV2 may become stronger versus LOV1-kinase or LOV2-kinase, leading to kinase activation only when both domains reach the adduct state and dissociate from the kinase. Another mechanism derived from observations of *Arabidopsis thaliana* in 2005 demonstrates the kinase being impeded from activation by LOV1.[18] This model makes LOV2 necessary for the mechanism and kinase dissociation and activation is achieved only when LOV2 is excited. Another possible mechanism could be that autophosphorylation actually occurs by cross phosphorylation whenever phototropins dimerize. Our goal for the experiments with LOV was to spectroscopically probe LOV-LOV interactions in dark and light states for the domains of the alga *Chlamydomonas reinhardtii* and the bacteria *Rhodobacter sphaeroides* and gain further understanding into the mechanism for how kinase activation and signal propagation may occur.

1.2) Förster Resonance Energy Transfer (FRET)

Förster Resonance Energy Transfer (FRET) is a non-radiative transfer of energy from a donor to an acceptor. Considered a spectroscopic ruler, it is used frequently when studying biological samples (e.g., proteins and membranes) to determine distances between donor and acceptor chromophores.[19] FRET occurs when a donor species, initially in the ground state, absorbs a photon and is taken to an excited state. The process of FRET competes with other non-radiative processes, (e.g., quenching) and radiative processes. The rate of energy transfer for FRET is related to the rates of competing processes through equation 1.2.1,

$$k_{transfer} = (k_{rad} + k_{nonrad})\left(\frac{R_0}{R}\right)^6 \qquad \textit{Eq. 1.2.1}$$

where $k_{transfer}$, k_{rad}, and k_{nonrad} represent the energy transfer rate, the radiative rate from the donor and all other non-radiative decay rates from the donor excited state, respectively.[20] R is the distance between the donor and acceptor while R_0 represents the Förster distance, the distance at which the rate of FRET is equal to the sum of all other rates possible from the decay of the excited state donor.

The relationship between the Förster distance (R_o) and the spectroscopic properties of donor and acceptor molecules may be seen in the equation for the Förster distance (equation 1.2.2).[20]

$$R_0^6 = \frac{9000(ln10)\kappa^2 Q_D J}{128\pi^5 n^4 N_{av}} \qquad \textit{Eq. 1.2.2}$$

In equation 1.2.2, κ^2 is an orientation factor representing the relative orientations of the transition moments for the donor emission and acceptor absorption, Q_D is the quantum yield of the donor molecule, J is the overlap integral, n represents the refractive index of the medium containing the donor and acceptor, and N_{av} is Avogadro's number. The overlap integral (J), describes the overlap of the donor emission and acceptor absorption spectra (equation 1.2.3).[20]

$$J = \int_0^\infty f_D\,(\lambda)\varepsilon_A(\lambda)\lambda^4 d\lambda \qquad \textit{Eq. 1.2.3}$$

Lambda (λ) is the wavelength of light, $\varepsilon_A(\lambda)$ is the acceptor molecule's molar absorptivity at such wavelength, and $f_D(\lambda)$ is the donor's normalized emission spectrum (equation 1.2.4), where $F_{D\lambda}(\lambda)$ is the emission of the donor per wavelength range.[20]

$$f(\lambda) = \frac{F_{D\lambda}(\lambda)}{\int_0^\infty F_{D\lambda}(\lambda)d\lambda}_D \qquad \textit{Eq. 1.2.4}$$

For a specific distance between donor and acceptor molecules, a specific energy transfer efficiency occurs. This efficiency, also called the FRET efficiency (equation 1.2.5), is the quotient of the energy transfer rate divided by the total of all rate transfer processes from the excited state of the donor.[20]

$$E = \frac{k_{transfer}}{k_{transfer} + k_{rad} + k_{nonrad}} \qquad \textit{Eq. 1.2.5}$$

The FRET efficiency can also be calculated from measuring the fluorescence intensity (F) of each FRET dye and knowing each species' quantum yield (θ) as seen in equation 1.2.6.

$$E = \frac{\frac{F_A}{\theta_A}}{\frac{F_A}{\theta_A} + \frac{F_D}{\theta_D}} \qquad \textit{Eq. 1.2.6}$$

The FRET efficiency can also be related to the distance (R) between FRET pairs via equation 1.2.7.[20]

$$E = \left(\frac{R_0^6}{R_0^6 + R^6}\right) \qquad \textit{Eq. 1.2.7}$$

1.2a) Single Molecule FRET Spectroscopy

When taking ensemble measurements, data from multiple sample molecules are averaged together. While there is benefit to ensemble measurements, subpopulations of molecules exhibiting different behaviors are missed with such approaches. In cases where biomolecular conformations and dynamics are observed, it is important to know whether a subpopulation exists and understand how it may affect the system studied. Therefore, single molecule measurements provide an avenue to explore such issues.

FRET has been used previously to study the conformations and dynamics of biomolecules.[21, 22] In such cases, FRET donor and acceptor molecules are chemically attached to different areas of the same protein or with donor and acceptor pairs attached to different proteins altogether. Whenever the protein changes conformation or separate proteins interact, the distance between donor and acceptor changes and, therefore, so does the FRET efficiency.

Notably, techniques such as single molecule burst measurements have been implemented to record the FRET of single molecules.[23, 24]

1.2b) Single Molecule Spectroscopy for Detecting FRET Bursts

In single molecule burst spectroscopy, fluorescence measurements are recorded from the donor and acceptor molecules as an individual molecule passes through the focal volume (~2 fL) of a laser focused by a microscope objective. During a typical experiment, an analyte in the picomolar range (10-100 pM, typically) repeatedly diffuses through the focal volume of the laser, with shot noise and background being detected when no analyte is present in the focal volume. Whenever the sample analyte passes through the focal volume of the focused laser, a sudden burst of fluorescence emission occurs and is recorded by the detectors.

For this work, we analyzed the collected fluorescence measurements for FRET between mixtures of donor and acceptor labeled samples of LOV domains using a photon distribution analysis program that incorporates maximum entropy methods.[25] The output of such analysis are probability distributions of the apparent FRET efficiency. This distribution is then used to compare the dark and light adapted states of the LOV domain sample mixture and determine, based on the changes in FRET efficiency, whether LOV domains are interacting.

Chapter 2- Single Molecule Burst Data

2.1) Rhodobacter sphaeroides

2.1a) Experimental

Sample Preparation:

Expressed LOV wild type with an N-terminal six-histidine tag from *Rhodobacter sphaeroides* (*Rsp*) was labeled via NHS-ester coupling with cyanine 3 (Cy3; FRET donor) or cyanine 5 (Cy5; FRET acceptor) dye (GE Healthcare Lifesciences) by our collaborators at the University of Regensburg in the Dick Lab. The labeling was confirmed via mass spectrometry for each labeled sample, with peaks identifying singly (22,080 Da) and doubly (22,692.0) labeled monomers for Cy3 bound *Rsp* (figure 2.1.1). Cy5 labeling was also confirmed via mass spectrometry to have been successfully bound to *Rsp* LOV, with peak values corresponding to singly (22,105.6 Da) and doubly (22,744.8 Da) labeled protein. However, only in the spectrum for *Rsp*-Cy3 were there peaks displaying dimers of *Rsp* that were unlabeled (~42,934.4 Da) or dimers composed of an unlabeled *Rsp* and a doubly labeled *Rsp* (44,159.2 Da).

Once it was confirmed by our collaborators that each respective aliquot was labeled, the samples were dialyzed in PBS (50 mM sodium phosphate, 10 mM NaCl, 0.1 % NaN_3, pH 7.2) prior to shipping. The spectra in figure 2.1.1 were collected at facilities at the University of Kansas as a double check they were still viable for use after being shipped. PBS stock (10 mM NaCl, 10 mM Na_2HPO_4 pH 7.78) used to prepare solutions for data collection was filtered with 0.22 µm Millex™-GP syringe filter (EMD-Millipore) prior to use.

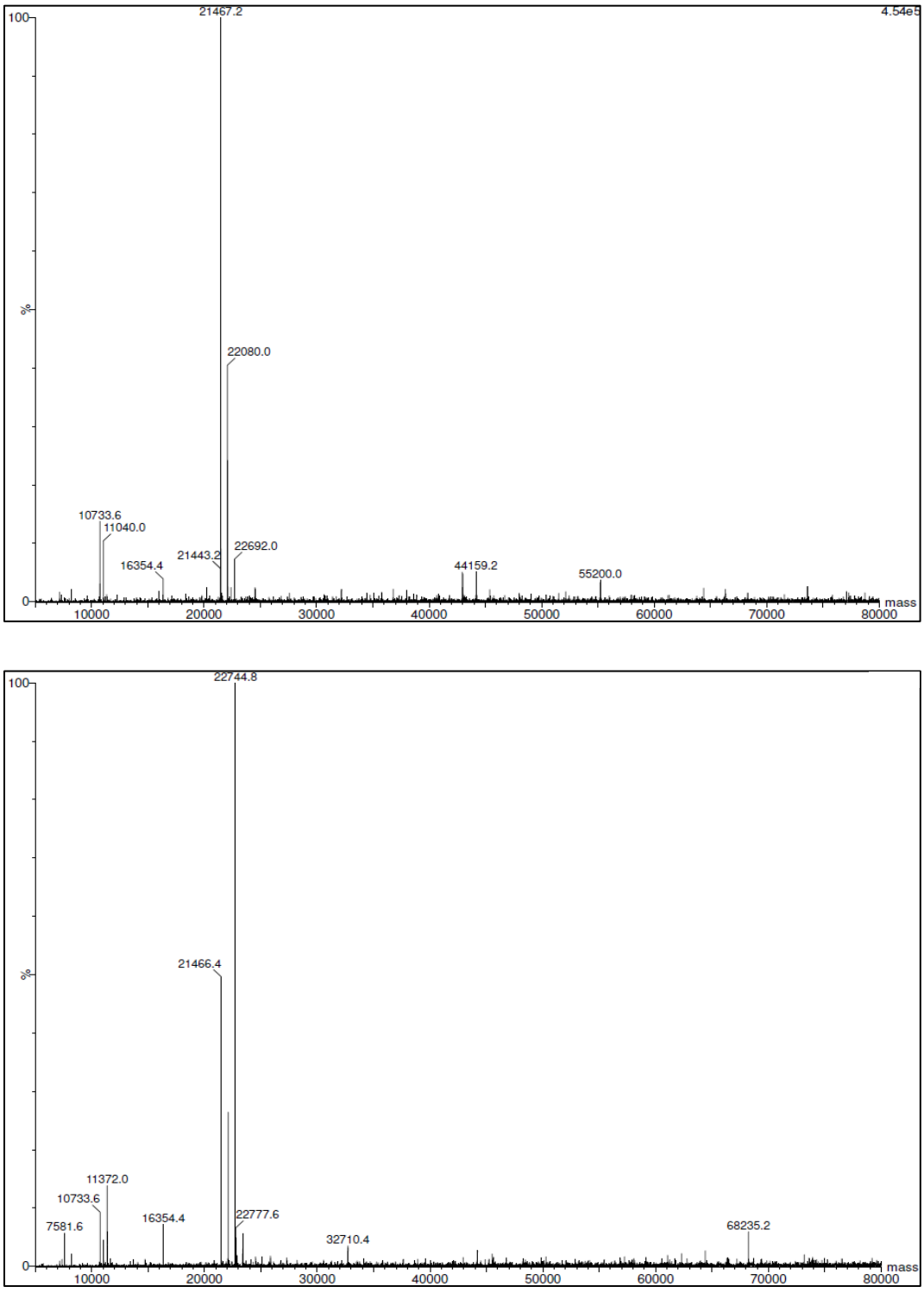

Figure 2.1.1- Mass Spectra for Rsp LOV wild type labeled with either cyanine 3 (top) or cyanine 5 (bottom). Samples were analyzed courtesy of the Analytical Proteomics Laboratory at the University of Kansas. Peaks corresponding to the masses of singly (Cy3: 22,080.0 Da, Cy5: 22,105.6 Da) and doubly (Cy3: 22,692.0 Da, Cy5: 22,744.8 Da) labeled Rsp show successful labeling of the protein.

For initial experiments with *Rsp*, the general scheme involved sample mixtures being dark adapted to heighten homodimerization of the proteins (e.g., Cy3-*Rsp*-*Rsp*-Cy3, Cy5-*Rsp*-*Rsp*-Cy5), then light adapted to cause dimer dissociation and form monomers (e.g., *Rsp*-Cy3 + *Rsp*-Cy3 + *Rsp*-Cy5 + *Rsp*-Cy5). Finally, the proteins were allowed to relax from their adduct state to form donor and acceptor labeled heterodimers (e.g., Cy3-*Rsp*-*Rsp*-Cy5).

To begin execution of this general scheme, labeled samples were mixed at equal concentrations (500 nM) and then diluted to 120 pM for a total volume of 4 mL in a glass bottom dish (part no. P35G-1.0-14-C; MatTek; Ashland, MA). All glass dishes that were used were rinsed immediately before sample was added with 1 mL PBS.

Once the sample mixture was diluted and placed in the glass bottom dish, it was allowed to equilibrate in the dish for ~20 minutes in the dark prior to data collection. Immediately following dark state data collection, preparation for the collection of light state data began with the same sample used for the dark state being repeatedly exposed to blue light for 10 seconds with a handheld LED lamp system (XR-E, Cree lighting; 450nm) constructed in our own lab. After 2 consecutive minutes of data collection, the sample was again exposed to blue light for 10 seconds. This process of repeated light exposure continued for the duration of the total data collection time. To measure the dark state reversion, the same sample used for the dark and light state measurements was left in the dark for ~40 consecutive minutes immediately following the conclusion of light state experiments. After ~40 minutes, data collection for the dark state reversion then resumed. After completing all measurements for the sample, background contributions were measured using a new dish and a fresh 4 mL aliquot of PBS only. The dish was prepared and rinsed in the same manner as the dish used for data collection with the sample.

To validate results, and based on information from our collaborators, further experiments were performed on two separate aliquots of sample mixtures, and each had its own specific experimental parameters. For what was identified as experiment #1, labeled donor and acceptor *Rsp* were combined to give equimolar concentrations (7.5 µM each) of donor and acceptor labeled proteins. Then, the sample mixture was left in the dark at least 5 hours before being diluted to a working concentration of 120 pM. The increase in time for leaving the sample mixture in the dark versus the incubation time in the initial experiments was done to maximize the number of *Rsp* proteins that dimerized. After the minimum 5 hour dark state incubation period, data was then collected for the sample mixture of experiment #1.

For conducting experiment #2, a fresh separate sample mixture was created to generate the same initial equimolar concentrations as experiment #1. However, experiment #2 differed in that the sample mixture was exposed to blue light for 8 minutes prior to its 5 hour minimum wait in the dark at 7.5 µM. The increased exposure time versus our initial experiments with *Rsp* was to ensure as many dye labeled proteins as possible would be excited to the adduct state, thereby enhancing the pairing of donor and acceptor labeled *Rsp* upon rearranging back to dimers in the dark. After the 5 hour minimum incubation period in the dark, the sample mixture was diluted to a working concentration of 120 pM and data was collected the same as for experiment #1.

In order to prevent protein adsorption in both experiment #1 and #2, each experiment's separate glass bottom dishes were incubated, before adding any sample, with 2 mL PBS (pH 7.18) containing bovine serum albumin (BSA, 2 mg/mL) for 5 minutes and immediately then dried with N_2 gas. The background was collected using a new dish that was incubated with a fresh BSA

solution aliquot and then dried with N_2 gas. A total volume of 4 mL of fresh BSA solution aliquot was used for background collection.

Burst Measurements for Determination of FRET efficiency and Dissociation Constant

To attempt to determine the dissociation constant for *Rsp* LOV dimers, a series of donor-acceptor labeled mixtures (30 nM-10 µM each) were prepared by mixing the labeled samples to 2x the desired concentration. This was done so that we would have the desired concentration of sample mixtures after combining Cy3 labeled samples with Cy5 labeled samples. PBS (pH 7.18) was used for each dilution of sample mixture. Each mixture was simultaneously exposed to blue light for 8 minutes before waiting at least 2 hours in the dark prior to measuring the fluorescence. Microscope slides (cat. no. 12-548C; Fisher Scientific; Pittsburgh, PA) were incubated with BSA solution (2.0 mg/mL) in the same manner previously mentioned with single molecule burst data. One hundred and twenty microliters of one of the diluted sample mixtures (now at 1x of the desired concentration) was placed over the treated portion of the slide and data was collected in ~1 minute increments. With assistance from an undergraduate researcher, Adebayo Braimah, multiple measurements were taken at one location on the slide and multiple locations were sampled per slide in order to minimize localized heating of the sample. Laser excitation power had to be adjusted per sample so as not to damage the detectors with high count rates (>250,000 counts per second). A fresh slide was prepared for each different sample concentration value and for background solutions, which were either PBS only or BSA in PBS solution. For determining the dissociation constant of *Rsp* LOV dimers, the net average acceptor to donor (A:D) ratio of photon counts was calculated and plotted versus the concentration of each sample.

Data collection and analysis

Burst Measurements for Determination of FRET Efficiency and Dissociation Constant

All FRET experiments were conducted on an inverted fluorescence microscope system (figure 2.1.2). Donor dye was excited by a helium-neon laser beam (544 nm, Research Electro-Optics, Boulder, CO). Excitation light was circularly polarized and focused 40 μm above the surface of either the glass bottom dish or coverslip via a water immersion objective (UPlanSApo, Olympus, 60x/1.20) attached to a Nikon TE2000 microscope. Excitation light and fluorescence from the sample were separated by a T560lpxr dichroic beamsplitter (Chroma Technology, Rockingham, VT). Green and red emission was split with a ZT640RDC dichroic beamsplitter (Chroma Technology) and then passed through separate 100 μm pinholes before being focused onto the active area of an avalanche diode detector (SPCM-AQR-14, Perkin-Elmer). Each detector also had an emission filter to further remove unwanted photons (ET 600/75M for donor, HQ 675LP for acceptor, both from Chroma Technology). Generated TTL pulses were recorded with a time counter card (PCI-6602, National Instruments) and time stamped via an 80 MHz (12.5 ns resolution) generated frequency from one of the card's eight counters. Photon arrival times were ordered into 300 μs time bins and placed in a histogram. Signal histograms with total counts (donor plus acceptor channel) greater than 10 were deemed above background and designated for analysis. Apparent FRET efficiency plots were created by photon distribution analysis, using a maximum entropy algorithm developed previously by DeVore et al, and with background count rates entered manually in units of counts per bin (c/bin) and determined individually for the donor and acceptor channels.[25]

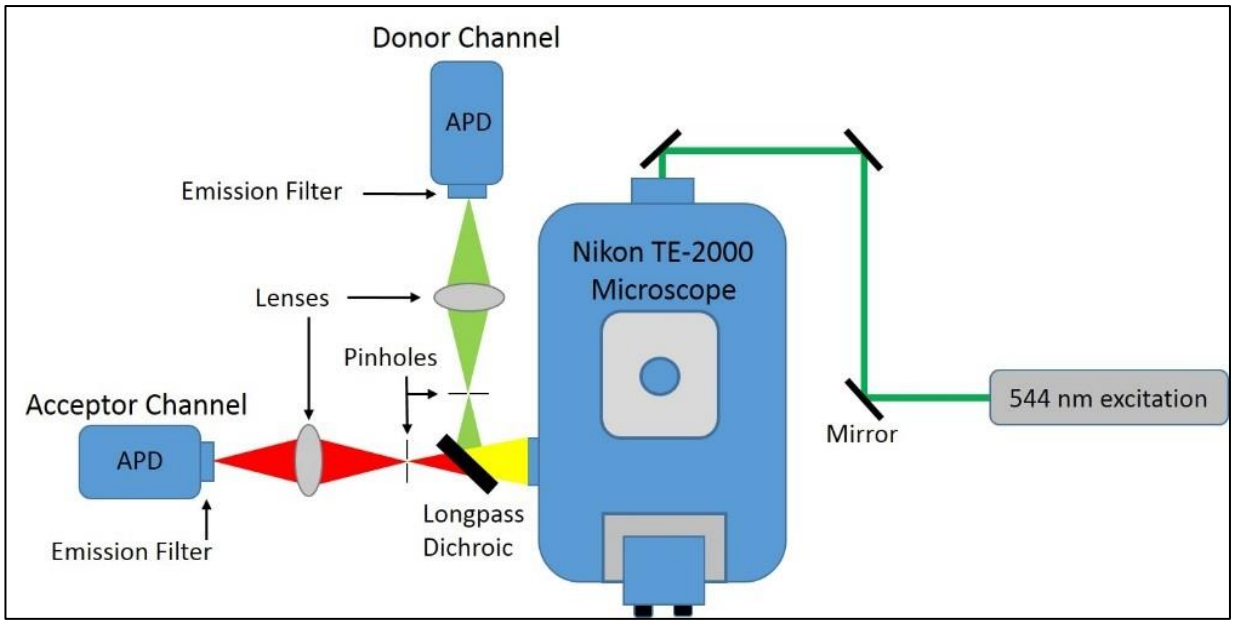

Figure 2.1.2- Schematic of two channel optical pathway for the detection of FRET via single molecule burst emission. Excitation light is directed up through the microscope objective to the sample. Emitted light is separated from the excitation prior to being split via a longpass dichroic to either acceptor or donor detector. Confocal pinholes (100 µm diameter) were used to remove unfocused light prior to reaching each detector.

2.1b) Results

The purpose of the single molecule burst measurements was to detect dimer formation amongst *Rsp* LOV dimers via a change in the apparent FRET efficiency. *Rsp* LOV differs from other variants in that dimers are favored in the dark state equilibrium, while monomers are favored after exposure to blue light. Presumably then, each aliquot of *Rsp* LOV each labeled with a single FRET dye (donor or acceptor) will favor homodimers in the dark. However when the aliquots are mixed, exposed to blue light, and then left in the dark, heterodimer formation should occur and the result between FRET pair labeled heterodimers will be an increase in the FRET efficiency.

For our initial experiments, figure 2.1.3 displays a FRET efficiency plot of wild type *Rsp* LOV before (Dark State) and after (Dark Reversion) blue light exposure. The burst data were

analyzed using a photon distribution analysis program written by Matthew S. DeVore. [25] This program uses a maximum-entropy algorithm for finding the probability distribution of the FRET efficiency. $P(E_{app})$ gives the probability to a corresponding apparent FRET efficiency (E_{app}). From the plot, it is observed that the peak probabilities for FRET are found at apparent FRET efficiency values below 10%, with minimal shift, if any, between dark state ($E_{app,max}$= 0.051) and dark reversion ($E_{app,max}$= 0.061).

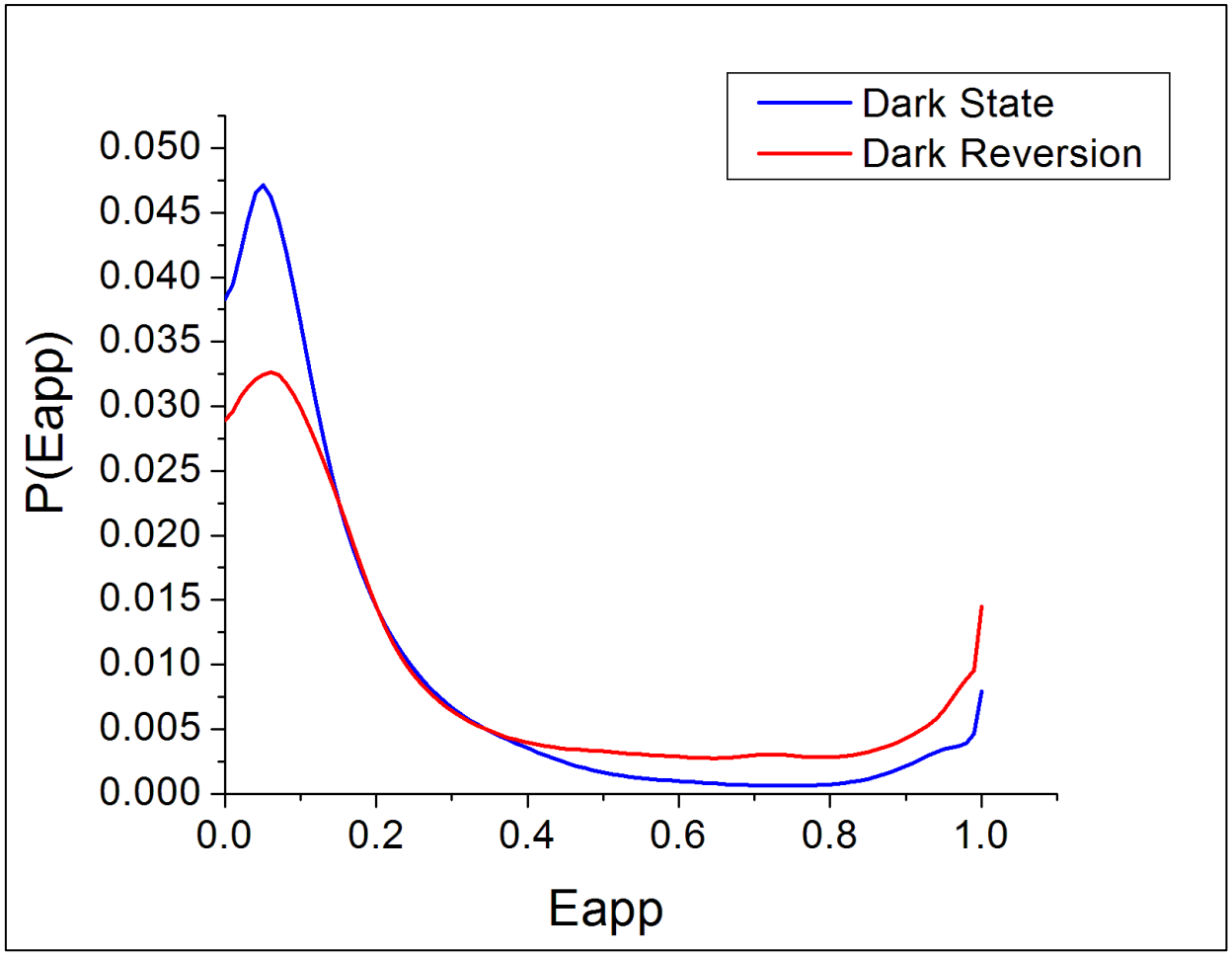

Figure 2.1.3- Apparent FRET efficiency plot of Rsp LOV wild type. Cy3 and Cy5 homodimers were at equal concentrations before being mixed (500 nM) and then diluted to the desired concentration of 120 pM. Once diluted to 120 pM, the sample mixture sat in the dark 20 minutes prior to measuring the dark state (blue). Samples were exposed to 450 nm blue light in 10 second intervals after every 2 minutes worth of data was collected. The sample mixture was left in the dark for 40 minutes after concluding the light state trial but before measuring fluorescence of the dark reversion state.

To validate our results from the initial experiments, we repeated the measurements but this time used two separate dishes each filled with their own respective sample mixtures so that they may be compared to each other. Figure 2.1.4 displays the apparent FRET efficiency plot for experiment's #1 and #2. In each experiment's case, 15 µM of donor *Rsp*-Cy3 was mixed with 15 µM *Rsp*-Cy5 to give each experiment sample mixtures of 7.5 µM donor and acceptor labeled *Rsp*. The key difference between the experiments is that experiment #1 never had the sample mixture exposed to blue light before incubating in the dark at least 5 hours. Experiment #2 did have the sample mixture exposed to blue light (8 minutes total) before its 5 hour minimum wait in the dark. Both samples were left in the dark at least 5 hours at 7.5 µM to ensure that there was enough time for the adduct to recover back to the ground state, which has been shown to be over 2000 seconds.[26] We were also questioning whether a more definitive change in the apparent FRET efficiency could be observed with greater exposure time to blue light, hence why we length of exposure to 8 consecutive minutes. Compared to the initial experiments with LOV *Rsp* wild type, the difference in the apparent FRET efficiencies for the dark and dark-reverted states appears to be greater with $E_{app,max}$= 0.061 for experiment #1 and $E_{app,max}$= 0.081 for experiment #2 (figure 2.1.4). Also, the $P(E_{app})$ for the initial experiments appears to be different, for in figure 2.1.4 the dark state reverted sample mixture (experiment #2) has a higher $P(E_{app})$ than for experiment #1 on the same plot. Both experiment #1 and #2 in figure 2.1.4 also appear to have greater overall maxima for $P(E_{app})$ values versus the maxima for $P(E_{app})$ in the initial experiments (figure 2.1.3).

The results regarding the apparent FRET efficiency performed initially on *Rsp* (figure 2.1.3) prompted questioning whether our experimental methods had allowed adequate amounts of

heterodimers to form. The concentrations needed to observe single molecule bursts are between 10^1 to low 10^2 pM. Such concentrations may be below the dissociation constant (K_d) value for *Rsp* LOV. It should be noted that, to our knowledge, no K_d value was known for *Rsp* LOV wild type. We decided to investigate this question by attempting to determine the dissociation constant for *Rsp* LOV wild type.

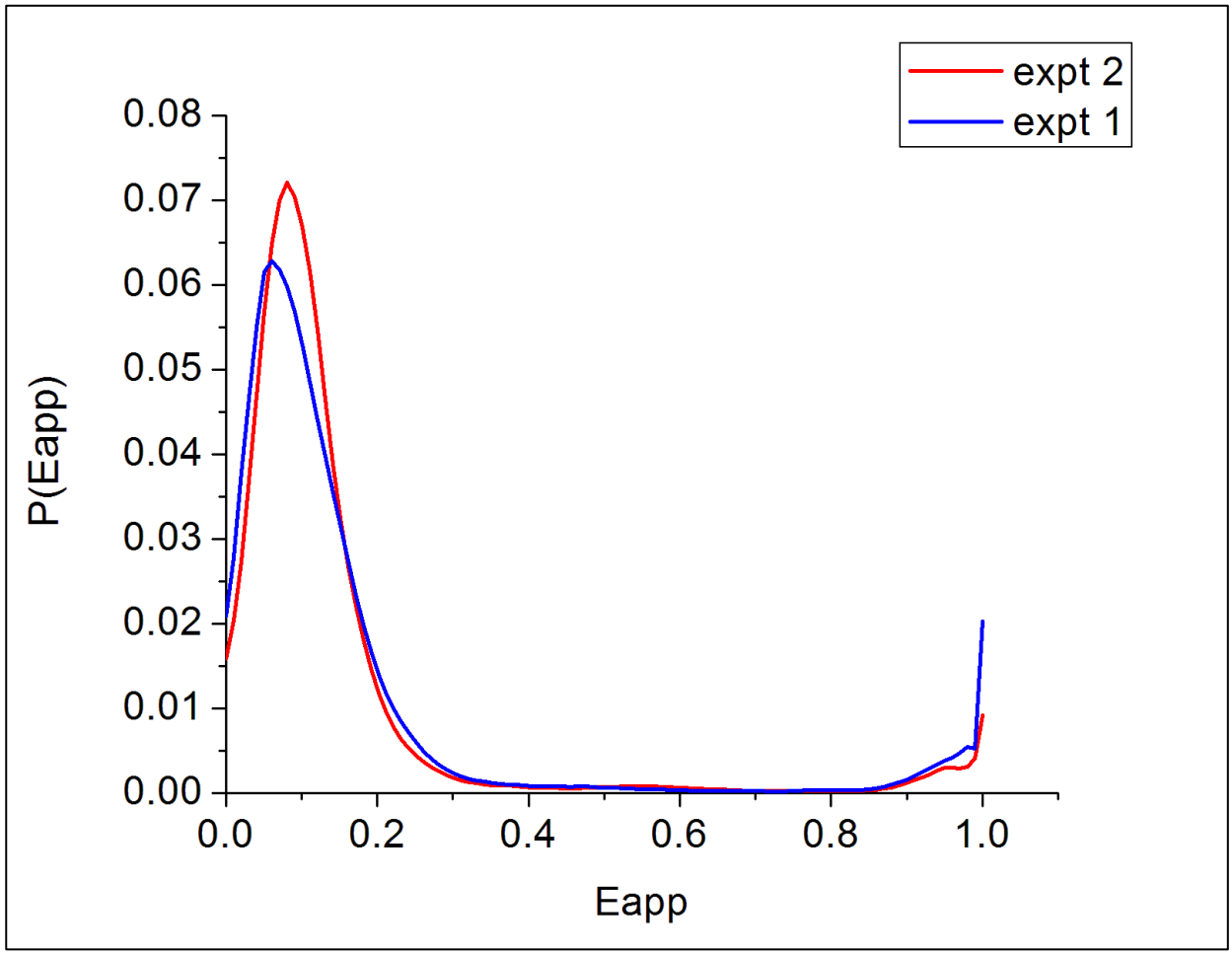

Figure 2.1.4- Apparent FRET efficiency plot of Rsp LOV wild type performed with greater mixing concentrations, longer blue light exposure times, and incubation for the dark state reversion. Experiment #1 (blue) had the sample mixture in the dark state, while experiment #2 (red) was exposed to blue light and was readapted to the dark state. Both experiments had the same concentration (15 µM) of donor and acceptor labeled Rsp LOV mixed in equal volumes to give 7.5 µM sample mixtures when incubating in the dark. Experiment #1 never had the sample mixture exposed to blue light before incubating in the dark at least 5 hours. Experiment #2 did have the sample mixture exposed to blue light (8 minutes total) before its 5 hour minimum wait in the dark. After the minimum 5 hour dark wait, each experiment's sample mixture was diluted 120 pM and fluorescence was measured.

Upon mixing, exposing to blue light, and then dark readapting, donor and acceptor labeled *Rsp* LOV will still achieve a ratio of monomers:dimers, but the value of the ratio is expected to depend on the concentration of the proteins in solution relative to the K_d value for *Rsp* LOV. When readapted to the dark at equilibrium, sample mixture concentrations at values less than K_d will shift the equilibrium toward monomer formation. In the case of *Rsp* LOV, that means less FRET should be observed. However, for sample mixture concentrations above the K_d, the ratio is expected to shift toward dimer formation, meaning an increased incidence of FRET for mixtures of *Rsp* LOV. Using the same dual channel microscopy setup as for the initial experiments, we were able to determine the net ratio of the number of photons detected in the acceptor channel versus the donor channel (net A:D ratio) for each sample mixed at a particular concentration of donor and acceptor labeled *Rsp* LOV.

Figure 2.1.5 gives a plot of the net average A:D ratio versus the working concentration of the sample mixture. A log scale was used for the x-axis for ease of viewing. Each data point is an average (n=5) of ~1 minute collection runs taken at a specific location on the microscope slide, for each concentration of the sample mixture applied to the slide for study. The average background counts (n=5) of acceptor and donor channel photons were subtracted from the total photons detected for each respective channel and for each collection run in order to attain a net value of photon counts for each detection channel. The net counts in the donor and acceptor channels per collection where then used to calculate the quotient for the net A:D ratio per collection run. Then, 5 collection runs taken at the same location on the slide and performed using the same excitation laser power were averaged to generate the net average A:D ratio. Points possessing the same x-axis values had their data collected on the same concentration of

sample and on the same microscope slide, but at different locations on the slide. It should be noted that the order by which samples were tested went from lowest concentration (30 nM) to highest concentration (10 µM), and that counts from the acceptor channel declined over the complete series of measurements for 30 nM *Rsp* LOV. This drop in counts could be attributed to photobleaching or some other photoinduced event. Also, a time component to the data may be observed at the 100 nM concentration, with the net avg. A:D ratio decreasing with each new slide position. A decrease in net average A:D may also be observed between the 250 nM and 750 nM values.

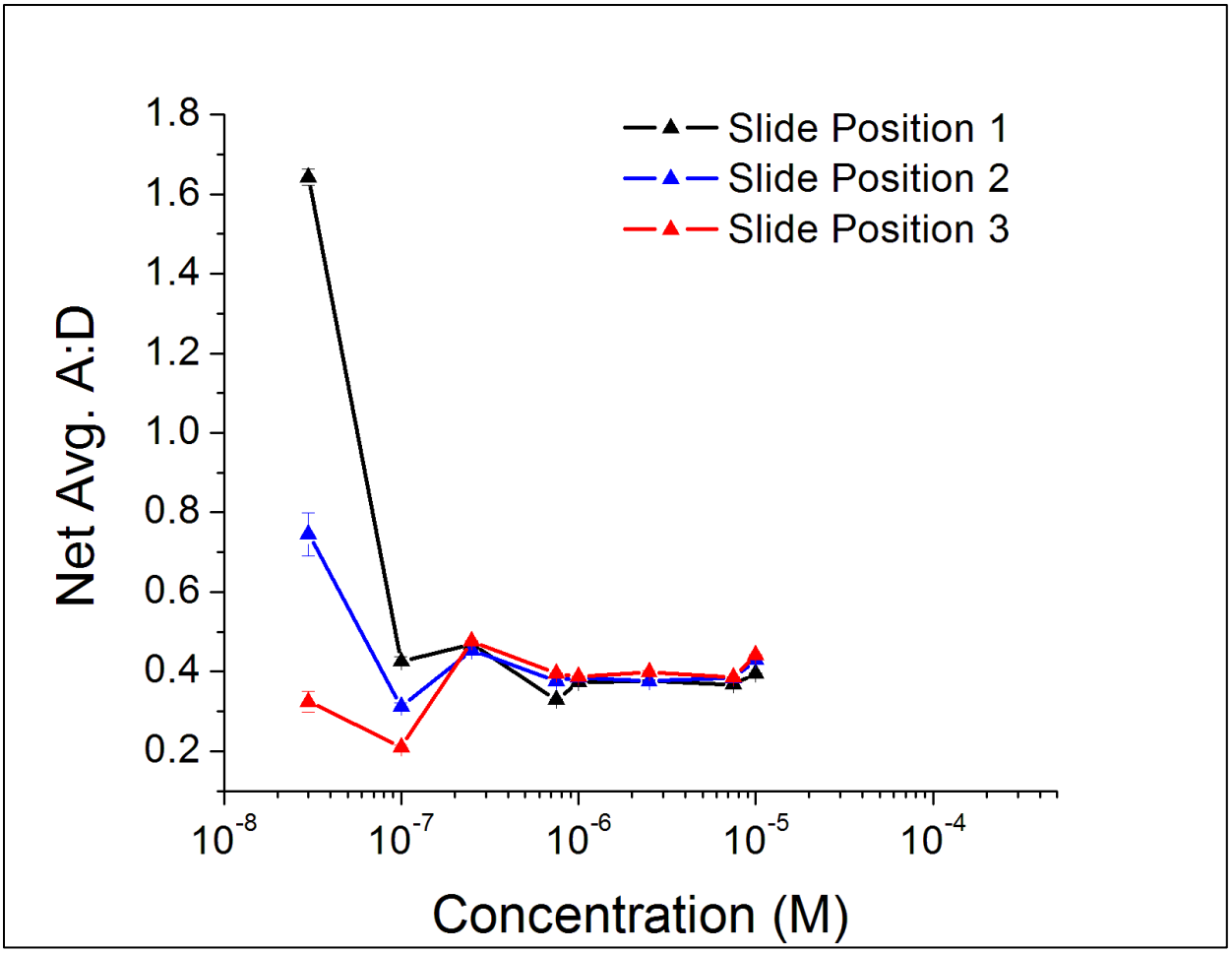

Figure 2.1.5- Plot for the determination of the dissociation constant for Rsp LOV wild type. Each data point (n=5) is the net average. A log scale was used on the x-axis for ease of viewing the data points at each concentration (30 nM, 100 nM, 250 nM, 750 nM, 1 µM, 2.5 µM, 7.5 µM, 10 µM). All error bars were generated by calculating the standard deviation of the mean.

2.1c) Discussion

Single Molecule Burst Measurements for Determination of FRET Efficiency

Unlike LOV domains in many other species, *Rhodobacter sphaeroides* LOV domains favor dimer formation in the dark and monomer formation in the light state. While the photomechanism of several species of LOV domains has been studied and understood, the process of transmitting the sensory signal from blue light to downstream signaling mechanisms is not well understood. The regulation of LOV domains forming dimers and monomers may play a role in such signaling processes. We used single molecule burst techniques to gain information about the interaction of LOV domains. Single molecule spectroscopy allows for measurement and detection of populations of states of molecules that otherwise would be overlooked in ensemble averaging measurements. To our knowledge, no single molecule burst measurements have been performed on *Rsp* LOV domains. The phenomenon of Förster Resonant Energy Transfer was used to detect the interaction of LOV domains. Since two different aliquots of *Rsp* LOV wild type were labeled with either donor or acceptor dye, it is only when a donor and acceptor labeled sample is mixed that FRET can occur. We used a method previously developed in our laboratory that takes advantage of classical maximum entropy to determine the most probable description for all detected photons emitted by fluorescence of the sample and the probability distribution for apparent FRET efficiency.[25]

The apparent FRET efficiency plots in figures 2.1.3 and 2.1.4 for *Rsp* LOV wild type perhaps demonstrate that there is a detectable difference between dark and dark adapted *Rsp* LOV based on the change in FRET. However, to see the change, a higher concentration of sample mixture after blue light exposure, along with longer waiting periods in the dark and more continuous blue

light exposure beforehand, may be needed. From figure 2.1.3, a minimal, if any, change in the peak value of E_{app} may be seen from the apparent FRET efficiency plot. In figure 2.1.4, there is a more noticeable shift in the peak value of E_{app}. Comparing figure 2.1.3 and figure 2.1.4, it makes sense that a greater change in FRET would occur if the sample mixture incubated at a higher concentration in the dark. In figure 2.1.3, sample mixtures were incubated in the dark state at 120 pM before being exposed to blue light. At a concentration potentially lower than the dissociation constant, the sample mixture would have a lower dimer:monomer ratio in the dark. A lower concentration of formed dimers means there would be a lower concentration of heterodimers formed in the dark reversion state and thus less overall FRET. Conversely, figure 2.1.4 had sample mixtures incubate in the dark prior to light exposure at a concentration of 7.5 µM each for the donor and acceptor. If this concentration was above the dissociation constant for *Rsp* LOV, then the ratio would shift towards more dimers. Upon being left in the dark again, greater amounts of heterodimers would form and a greater amount of FRET could be seen.

Another possible factor for increasing FRET between labeled *Rsp* LOV may have been the longer, more continuous period of blue light exposure, followed by an extended period for the sample mixture to recover in the dark state. Longer periods of blue light exposure would shift the equilibrium to favor monomers even more versus shorter periods of blue light exposure. Allowing the sample to recover in the dark longer than the adduct decay time would enhance more heterodimer formation than interrupting dimer formation with short periods of blue light exposure.

The preceding statements also could help to account for the shape of the curves in figure 2.1.3 versus figure 2.1.4. Since figures 2.1.3 and 2.1.4 are normalized probability distributions,

any loss in $P(E_{app})$ in one area of a curve will be compensated by an increase in the $P(E_{app})$ in another area of the curve. In figure 2.1.3, the peak maximum for the dark reversion state may be decreased in value for $P(E_{app})$ versus the dark state, but $P(E_{app})$ for the dark reversion curve increases and becomes greater than the dark state's $P(E_{app})$ value for E_{app} > (~0.4). This could indicate *Rsp* LOV is forming dimers or even oligomers; however, the difference in the values is small and may not be significant. The same trend at higher values of E_{app} is not observable in figure 2.1.4. If oligomers formed while keeping the *Rsp* sample mixture in the dark for 40 minutes after briefly (every 2 minutes for 10 s) exposing them to blue light (figure 2.1.3, dark reversion curve), then greater amounts of oligomers could form when a higher concentrated sample mixture is exposed to longer, more continuous periods of blue light and incubated much longer to reacquire the dark state dimer to monomer ratio. The apparent FRET efficiency plots would reflect this by continuing to shift to higher values of E_{app}, and thereby decreasing the height of the peak at lower E_{app} values. However, this trend is not observed in figure 2.1.4, thereby making it possible the rise in figure 2.1.3 at higher E_{app} could be an artifact.

Determination of Dissociation Constant

We originally began attempting to determine the dissociation constant for *Rsp* LOV wild type because we were concerned our concentrations needed for single molecule burst measurements (120 pM) was causing an equilibrium shift that favored monomer formation. Knowledge about the K_d value would be useful for designing future experiments to understand the dynamics of the protein. Before the data analysis we were expecting the plot of net average A:D ratio vs concentration to give a sigmoidal curve, with a dramatic increase in the ratio for determination of the dissociation constant. However, the plot displays a varied ratio at lower

concentrations. At lower concentrations, net average A:D ratios appear to decrease over time. At higher concentrations than 100 nM, the plot stabilizes and does not present a shift in A:D that allows determination of the $K_{d.}$ However, when examining the net average A:D ratios, we wondered whether the values calculated demonstrated that FRET was occurring because of heterodimer formation. We calculated the contribution to the A:D ratio by direct excitation of the acceptor dye cyanine 5 and detector cross talk to be 0.057. From figure 2.1.5, we observed no data points with net average A:D ratios below (~0.2). This means that despite not being able to determine a K_d value for *Rsp* LOV wild type, we do demonstrate FRET that can be attributed to heterodimer formation after relaxation from the adduct state.

In summary, we used single molecule spectroscopy methods to probe the interactions of the LOV domain for *Rhodobacter sphaeroides.* We demonstrated seeing FRET within mixtures of *Rsp* donor and acceptor labeled LOV that was readapted to the dark state. The amount of FRET observed was enhanced by increasing the concentration of the sample mixture after being exposed to blue light, longer periods of blue light exposure, and longer waiting times in the dark before measuring fluorescence for the dark-reverted state. We also attempted to determine the equilibrium dissociation constant for *Rsp* LOV. However, despite detecting FRET from analysis of the net average A:D ratio that was not accounted for by cross talk or direct excitation of the acceptor, our data plot did not show a significant change in the net average A:D ratio necessary for determining a dissociation constant.

2.2) Chlamydomonas reinhardtii

2.2a) Experimental

Sample Preparation:

Single Molecule Burst Measurements for Determination of FRET Efficiency

LOV1 A16C C32S C83S expressed and purified by the Protein Production Group (Center of Biomedical Research Excellence, University of Kansas) and LOV1 A16C C32S C57G C83S (Bernhard Dick Lab Regensburg, Germany) from *Chlamydomonas reinhardtii* (*C.r.*) were labeled with cyanine 3 and 5 dyes (GE Healthcare Lifesciences) respectively via maleimide coupling chemistry and filtered by gravity flow chromatography (Sephadex™ G-25 GE Healthcare Life Sciences). Both proteins had their respective histidine tags cleaved prior to labeling and were dialyzed in filtered PBS (10 mM NaCl, 10 mM Na_2HPO_4 pH 8.0) to remove unbound dye after labeling. PBS stock was filtered (0.22 µm, Millex) before use.

Donor and acceptor samples were mixed at 500 nM each and subsequently diluted to 120 pM in 4 mL total volume in a rinsed glass bottom dish (MatTek). For both the initial and repeat experiment, the sample mixture sat in the dark for 20 minutes prior to measuring the dark state and at least 20 minutes prior to measuring the dark reversion in the repeat experiment. Light state measurements were taken in 2 minute increments, with 10 seconds of blue light exposure before collecting each data file. For the initial experiment, both the dark and light state measurements were collected for a total of 2 hours. In the repeated experiment, dark state, light state, and dark reversion state measurements were each collected for 1 hour of total time. To complete both the initial and repeat experiment, only 1 dish per experiment was used for each experiment's sample mixture. Data collection and analysis was conducted in the same manner as for *Rsp* samples in determining the FRET efficiency.[25] The initial and repeat experiment each

had background signal collected, with each experiment using a fresh PBS aliquot placed in a new glass bottom dish that was rinsed with PBS prior to collecting background measurements.

2.2b) Results

Similar to single molecule burst measurements with *Rsp* LOV wild type, our initial objectives were to observe the change in the FRET state when dark adapted mixtures of donor and acceptor labeled *Chlamydomonas reinhardtii* (*C.r.*) LOV were exposed to blue light. Unlike *Rsp* LOV, *C.r.* LOV forms monomers in its dark state, and then forms dimers in the light state (figure 2.2.1). Figure 2.2.2 displays a plot of the apparent FRET efficiency for a sample mixture of LOV1 A16C C32S C83S Cy3 and LOV1 A16C C32S C57S C83S Cy5 mixed at 500 nM each and then the resulting 250 nM mix was diluted to 120 pM for measurement. When exposed to blue light, the sample was already at 120 pM. Due to the contribution of detector cross talk in our instrument set up and direct excitation of cyanine 5, the peaks for $E_{app,max}$ would appear at 0.06 and not zero when only monomers are present. It was observed that the $E_{app,max}$ for both donor and acceptor was the same value (0.091). Each curve also has the same probability maximum (0.082 for dark state, 0.082 for the light state) and shape over the course of the entire plot region. This indicates that there is no difference in the dark and light states for the apparent FRET efficiency and that mostly monomers are presumed to exist in the sample mixture.

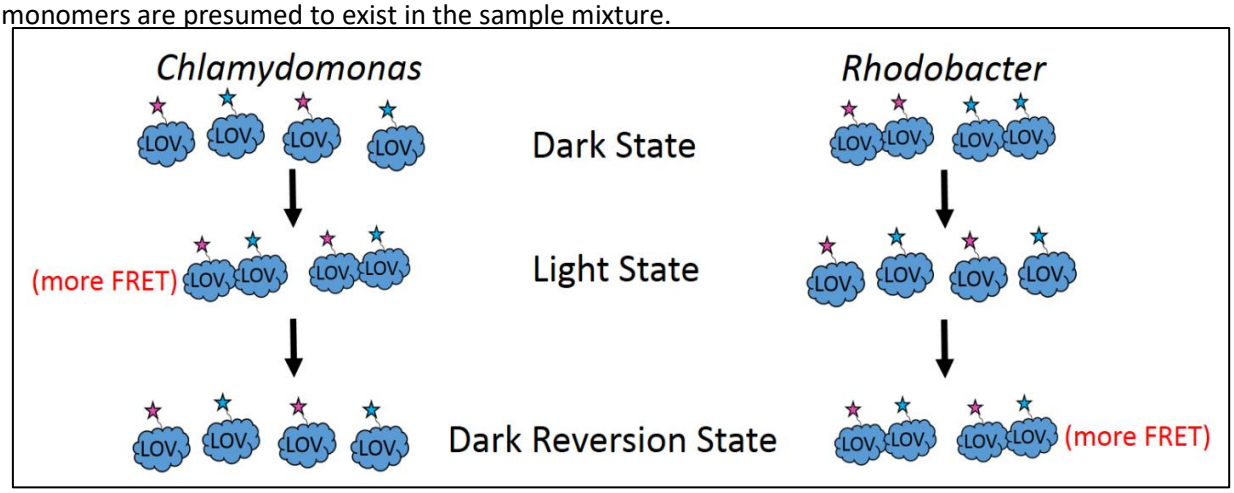

Figure 2.2.1- Schematic overview of how LOV sample mixtures from Chlamydomonas reinhardtii and Rhodobacter sphaeroides may interact when left in the dark (Dark State), exposed to blue light (Light State), and when allowed to incubate in the dark again (Dark Reversion State). Pink stars represent Cy3 (donor) dye that is covalently bound to LOV, while blue stars represent Cy5 (acceptor) dye covalently bound. For Chlamydomonas, dimerization is favored in the light state and we expect greater amounts of FRET there. However, Rhodobacter is expected to have greater amounts of FRET in the dark reversion state due to its LOV forming more dimers in the dark.

In order to monitor if the sample mixture of LOV1 A16C C32S C83S Cy3 and LOV1 A16C C32S C57S C83S Cy5 would produce similar results to the dark state reversion, we attempted a repeat experiment with a fresh sample mixture and background. Figure 2.2.3 is the apparent FRET efficiency plot for a fresh sample of the same type of LOV donor and acceptor labeled proteins used to generate figure 2.2.2. From the plot, it is observed that the peaks for the dark and dark reversion states (blue and red lines respectively) have almost the same value ($E_{app,max}$= 0.061 for dark state, $E_{app,max}$= 0.071 for dark reversion state) and that the dark state has the same $E_{app,max}$ as the light state.

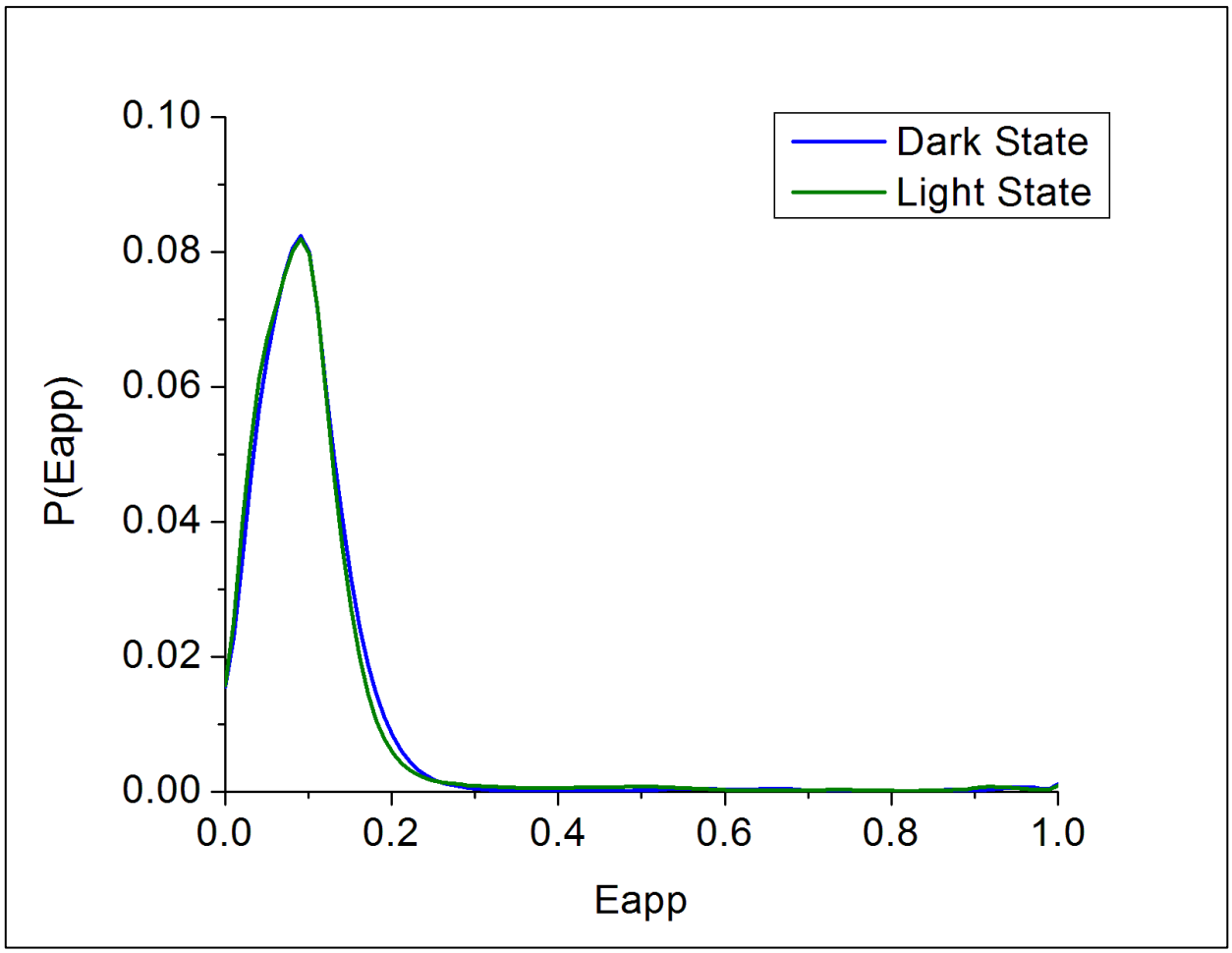

Figure 2.2.2- Apparent FRET efficiency plot of LOV1 A16C C32S C83S Cy3 and LOV1 A16C C32S C57S C83S Cy5 sample mixture. Donor and acceptor labeled proteins were mixed at 500 nM each and then diluted to 120 pM for each species. The mixture sat in the dark 20 minutes prior to measuring for the dark state. When exposed to blue light, the sample mixture had a concentration of 120 pM.

Due to the contribution of detector cross talk in our instrument set up and direct excitation of cyanine 5, the peaks for $E_{app,max}$ would appear at 0.06 and not zero when monomers are present. Figures 2.2.2 and 2.2.3 appear to show no change in the FRET state between the dark state, the light state, or the dark reversion state of the sample mixture.

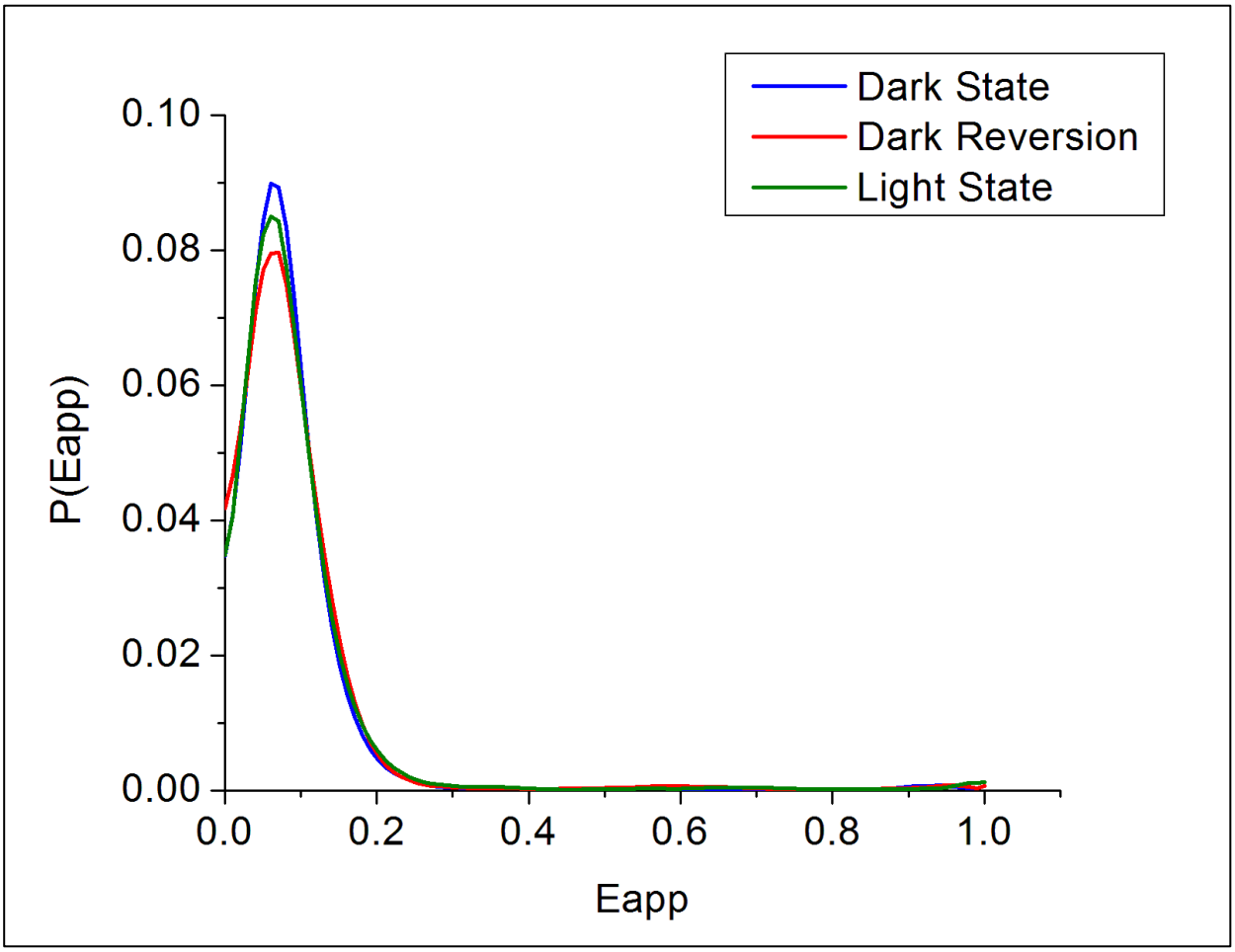

Figure 2.2.3- Apparent FRET efficiency plot for repeat experiment with fresh LOV1 A16C C32S C83S Cy3 and LOV1 A16C C32S C57S C83S Cy5.The sample mixture was allowed to sit in the dark for 20 minutes prior to measuring both the dark state and dark reversion state.

2.2c) Discussion

In contrast to *Rsp* LOV, LOV domains from the alga *Chlamydomonas reinhardtii* (*C.r.*) favor monomer formation in the dark and dimer formation when exposed to blue light. This means that for single molecule burst measurements on *C.r.* LOV, an increase in FRET efficiency should occur in the light

state and the FRET efficiency should decrease after equilibrium has been reached during reversion (figure 2.2.1). We performed single molecule burst experiments to determine whether we could in fact identify a change in FRET between the dark and light states. While we did notice that the dark reversion state did return to almost the same E_{app} as the sample mixture possessed in the dark state, we also noticed that the $E_{app,max}$ for the light state was similar to the dark and dark reversion states in both the initial and repeat experiment. Upon analysis we observed no noticeable change in the FRET efficiency between dark and light states of *C.r.* LOV1 (figures 2.2.2 and 2.2.3). However, this outcome was not totally unexpected.

Similar to experiments performed with LOV from *Rhodobacter*, the concentration of the sample mixtures for *Chlamydomonas* may be so far below the dissociation constant that minimal, if any, FRET is generated from heterodimers. It should also be remembered that in order to allow the conformational changes necessary for the dimerization of LOV domains, the protein must allow for a conserved cysteine residue to form a covalent bond with the flavin mononucleotide cofactor associated with each native *C.r.* LOV domain. In our *C.r.* domains labeled with Cy5, this conserved cysteine (at sequence site 57) was not present due to being mutated out of the sequence by our collaborators. By using a photoinactive mutant of the *C.r.* LOV1 domain when detecting for FRET, a lesser chance exists that the inactive domain will be in the most optimal conformation to bind to a donor labeled, photoactive domain, and thus decreasing the amount of change in FRET between the dark, light, and dark reversion states.

3) Stopped-Flow Spectroscopy

3.1) Background

In order to better understand the interactions between LOV domains, we wanted to know something about the timescales over which the events of interest would occur. LOV itself is an aqueous membrane protein that is photosensitive.[27] [28] Any spectroscopic experiments we designed had to account for the spectra of any reporter dyes bound to LOV, so that no contribution from the flavin will be present if FRET is observed. From previous literature, it is known that the dark state reversion process occurs on the order of tens to hundreds of seconds.[29] Therefore, a technique with second to sub-second resolution could be used to monitor the reaction. Stopped-flow spectroscopy is a well-known technique for determining kinetic parameters. First developed in the 1930's, this physical method consists of injecting at least two species for study into a mixing chamber and then monitoring the reaction over time within the chamber.[30, 31]

The goal of our experiments was to use stopped-flow techniques to monitor the light dependent interactions between LOV domains singly labeled with FRET dyes. By mixing two aliquots of LOV domains, each labeled with either a FRET donor or acceptor, we can monitor the amount of FRET occurring when the domains interact. Stopped-flow spectroscopy combined with FRET has been demonstrated in other biochemical investigations and is suitable for the timescales necessary for detection of LOV-LOV pairing.[32, 33] Previously, Kutta et al. had shown LOV1 wild type from *Chlamydomonas reinhardtii* (*C.r.*) has been observed with size exclusion chromatography to form only dimers and higher aggregates (>200 kDa) in the dark state, conflicting with previous studies by Federov et al.[15, 34] However, SDS-PAGE cross-linking studies

have demonstrated a ratio of 1.3 monomers to dimers in the dark that could be altered after exposure to blue light.[15] Data fits showed that the time constant for the recovery of the monomer/dimer ratio was on the order of 10^2 seconds.[15] If signal from the acceptor could be detected after blue light exposure, our findings would support light-induced interactions between LOV1 domains and would also provide the time constants over which such an interaction would occur.

3.2) *Chlamydomonas reinhardtii*

3.2a) Experimental

Sample Preparation:

Stopped-flow measurements for *Chlamydomonas reinhardtii* LOV1

Samples of histidine-tagged LOV1 (wild type, C83S, and C57G C83S mutants) were synthesized and purified by our collaborators at the University of Regensburg. With the assistance from an undergraduate researcher, Ashley McDade, the samples were labeled with either cyanine 3 or cyanine 5 dye by maleimide coupling chemistry. Free dye was separated from labeled samples by size exclusion chromatography by Sephadex G-25 media. Samples were checked for labeling by mass spectrometry and frozen as aliquots at -80^{o}C for future use.

General Stopped-Flow Experimentation

Frozen samples of donor and acceptor labeled LOV were thawed from the -80^{o}C freezer. Samples were dialyzed in PBS (10 mM NaCl and Na_2HPO_4 pH 7.0-7.4) overnight. Each sample solution was diluted to twice the concentration that would be used for taking measurements. The samples were then loaded into separate syringes, with each syringe wrapped in aluminum foil to prevent unwanted light exposure, and each was installed into its own injection port atop

a SX18 Stopped-Flow Spectrometer (Applied Photophysics, United Kingdom). With assistance from Ashley McDade, samples were diluted and mixed at equimolar concentrations. Within the mixing chamber, which was also covered in aluminum foil, the sample solution was then exposed to 550 nm light and emission from the donor and acceptor dyes was recorded via two separate photomultiplier tubes, each with its own respective filter (both from Chroma Technology Corp., donor channel: 590/50M; acceptor channel: HQ667LP) for removing excitation light and minimizing cross talk between detectors. Each detector had its response voltages set approximately between 6-8 volts in order to maximize signal response while staying below the maximum limit of 10 volts. For dark-state runs, samples were kept in the dark. For light-state experiments, samples in the injection syringes were exposed to blue light (450 nm) from a homemade, handheld LED lamp for five seconds. Between each run, the unmixed samples were again exposed to blue light, and the mixing chamber was flushed with fresh mixed solution 5 times prior to each trial. Plots of detector response versus time were generated and the raw data from the acceptor channel was curve-fit by Origin® 7 graphing and analysis software (OriginLab, Northhampton, MA). Samples were fit with a multi-exponential equation (equation 3.2.1), and each data curve was fit with as few number of exponentials as possible,

$$y = A_0 - A_1 e^{-t/\tau} - A_2 e^{-t/\tau} - \dots etc \qquad \textit{Eq. 3.2.1}$$

where A0, A1, and A2 are amplitudes, (t) is time, and τ is the time constant per each exponential component and represents the rate of appearance of FRET.

3.2b) Results

A sample mixture of LOV domains containing both donor and acceptor singly labeled monomers is not expected to generate FRET. However, the detection of FRET would indicate dimerization or even oligomerzation of domains had taken place. Figure 3.2.1 displays a plot of the donor channel (figure 3.2.1a, top left) and acceptor channel (figure 3.2.1b, top right) for a series of consecutive injection runs with the sample mixture being His-tagged LOV1 WT Cy3 and His-tagged LOV1 C57G C83S Cy5 in the dark state.

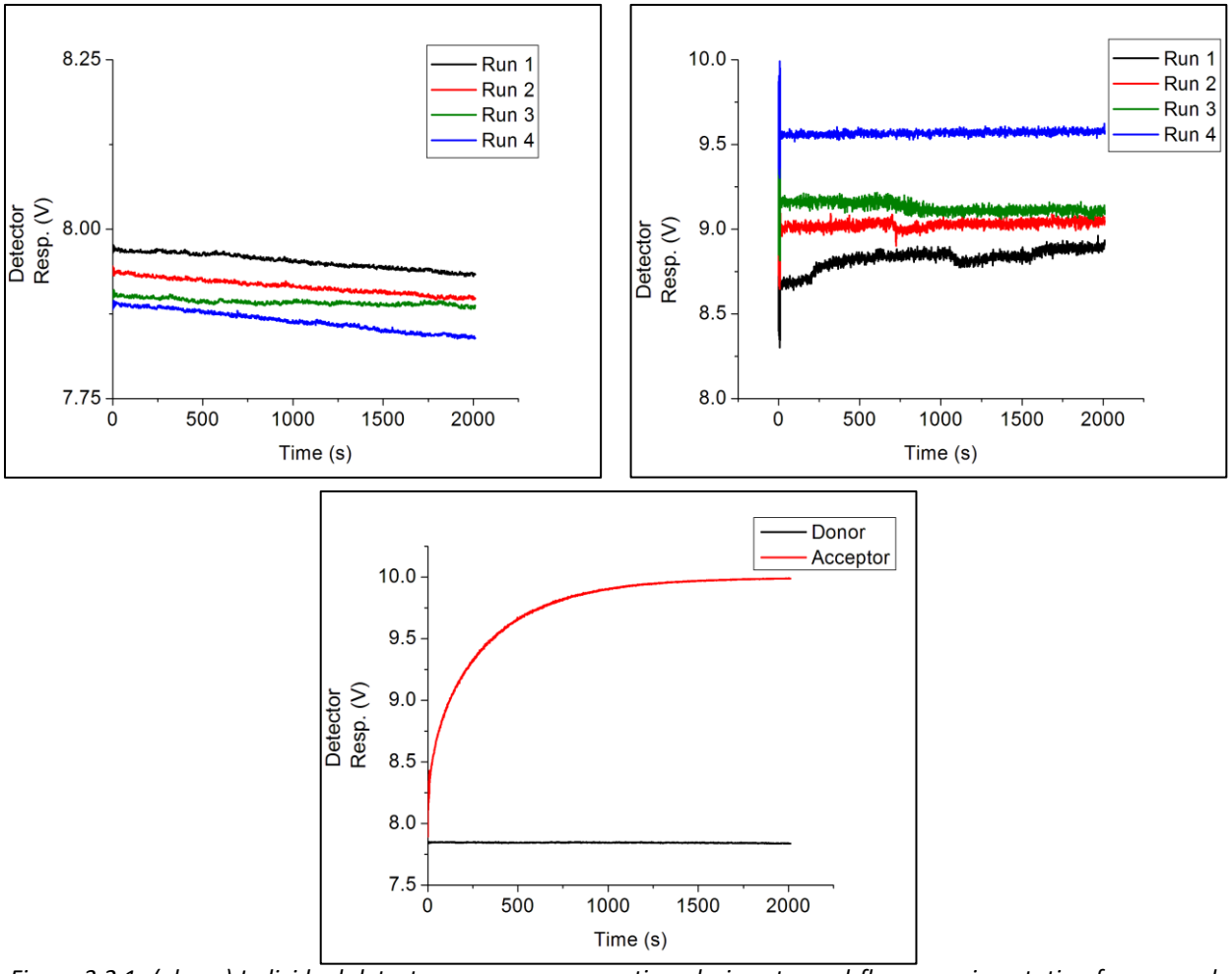

Figure 3.2.1- (above) Individual detector responses versus time during stopped-flow experimentation for a sample mixture of histidine tagged proteins LOV1 WT Cy3 and LOV1 C57G C83S Cy5. Figure 3.2.1a (top left) gives the detector response in the donor channel and figure 3.2.1b (top right) gives the detector response in the acceptor channel. The proteins were mixed and remained in the dark for the duration of each run, with the mixing chamber being injected with fresh sample mixture prior to each run. Upon blue light (450 nm; figure 3.2.1c, bottom) exposure, a distinct rise in the acceptor channel is observed via FRET between donor and acceptor labeled LOV1 dimers.

Figure 3.2.1c (bottom) gives the donor and acceptor channel responses to an injection of His-tagged LOV1 WT Cy3 and His-tagged LOV1 C57G C83S Cy5 after being exposed to blue light for 5 seconds. The difference in the initial voltages between the individual dark state runs in figure 3.2.1a and 3.2.1b can be attributed to detector drift over time, while the large spikes in noise, occurring only over the first 10 seconds of data collection (e.g., figure 3.2.1b), are caused by collecting more data points per second versus the remaining 2000 seconds. In figure 3.2.1a, we also noticed a decrease in signal over time for the donor channel, possibly indicating photobleaching. The negative slope seen in the donor channel makes sense for photobleaching given the time (2000 s) over which the sample in the mixing chamber is continuously exposed to light of 550 nm wavelength. Due to the setup of the mixing chamber within the stopped-flow spectrometer, samples had to be exposed to blue light *before* mixing.

Figure 3.2.2 gives the plots of detector response over time in the acceptor channel for the recorded runs of LOV1 WT Cy3 mixed with LOV1 C57G C83S Cy5 after being exposed to blue light. The plots in figure 3.2.2 were used to recover the time constants and relative amplitudes for each trial displayed in table 3.2.1. Note that the trials 1-3 are recorded on a separate day versus trials 4-7, hence they are shown on different plots. Figure 3.2.2 demonstrates that the slope of the initial portion of each curve becomes progressively less steep over each trial, which were performed in numerical order. This contrasts with dark state only experiments with LOV1 C83S Cy3 donor (figure 3.2.3), where the time constants appear relatively stable over multiple trials (all taken on the same day, table 3.2.2).

Upon the samples mixing after being exposed to blue light (450 nm), a sharp rise in signal is detected from the acceptor channel. Since the samples were exposed the blue light prior to mixing and only 550 nm excitation was used within the mixing chamber, any rise in signal above noise is caused by FRET between donor and acceptor labeled LOV.

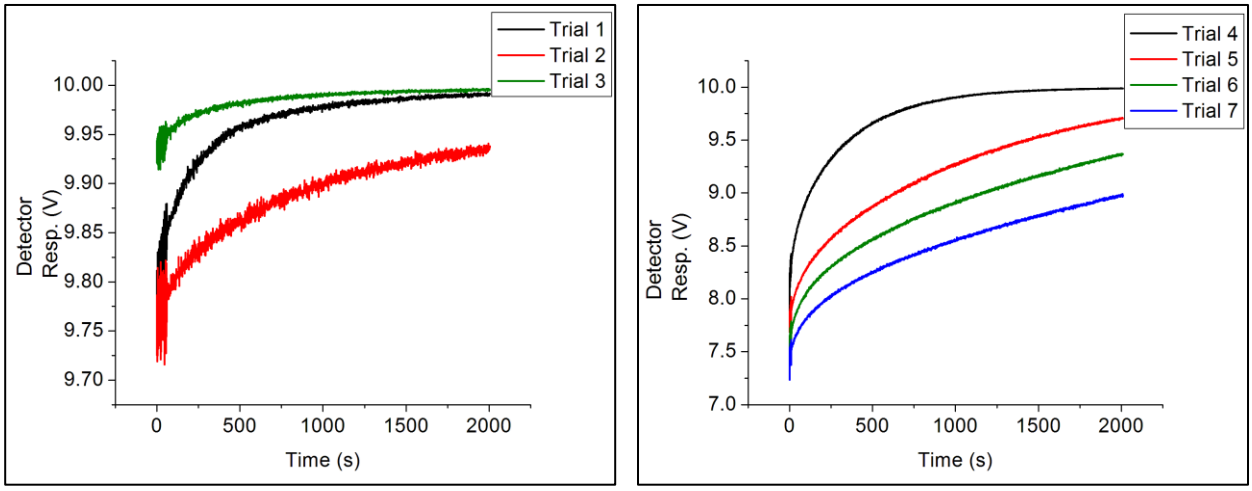

Figure 3.2.2- Detector response over time for light state mixture of LOV1 wild type Cy3 and LOV1 C57G C83S Cy5. All curves plotted on the same axes (Trials 1-3, 4-7) were performed on the same day. Due to an unexplained error in collecting the data, trial 3 was exempt from future analysis.

Table 3.2.1- Time constants (τ_1, τ_2) and relative amplitudes (A_1, A_2) *for FRET paired LOV1 wild type Cy 3 mixed with LOV1 C57G C83S Cy 5 after light exposure for 5 seconds prior to mixing. Curves for the acceptor channel were fit and trials shaded blue were taken on a separate day to repeat results.*

Trial	1	2	3	4	5	6	7	Avg. (1-7)
τ_1 (s)	85 ±4	96 ±7	110 ±8	23 ±1	58 ±1	62 ±1	77 ±1	73 ±3
τ_2 (s)	442 ±15	937±9	597 ±39	344 ±1	1110 ±8	1454±16	1741 ±4	946 ±13
A_1	0.094 ±0.003	0.040 ±0.001	0.029 ±0.002	0.43 ±0.01	0.43 ±0.01	0.46 ±0. 03	0.38 ±0.01	0.27 ±0.07
A_2	0.11 ±0.01	0.15 ±0.01	0.033 ±0.010	1.4 ±0.1	1.8 ±0.1	1.8 ±0.1	1.7 ±0.1	1.0 ±0.1

When analyzing curves collected from the light state, we found two-exponential fits to be suitable for fitting, with time constants on the order of tens to low hundreds of seconds (τ_1) and hundreds to low thousands of seconds (τ_2). Table 3.2.1 gives the recovered time constants for the light state, with the average of all seven trials. Trials 1-3 were actually performed on the same day, with trials 4-7 taken on a separate day versus trials 1-3.

For the two days' worth of experiments, it should be noted a trend may be observed in the individual plots of each trial. Table 3.2.1 displays that as each run progresses for each experiment set, there is an increase in the time constants for all trials (except trial 3). Prior to collecting for trial 3, a discounted trial displayed a large sloped increase in the donor channel, with an even greater increase near the ~100 second mark. Something could have gone wrong (e.g., detector power surge) in this rejected trial and may have carried over the problem to the accepted trial 3. For this reason, trial 3 will be excluded from future analysis.

Figure 3.2.3 gives the responses in the acceptor channel for recorded trials of LOV1 C83S Cy3 mixed with LOV1 C57G C83S Cy5 in the dark state. Similar to plots in figure 3.2.2, the individual plots of figure 3.2.3 possess a similar shape for the acceptor channel's detector response. However in figure 3.2.3, the trend of an increasingly shallow response curve with each successive trial collected is not present. Rather, each successive trial gives a curve that is translated to higher detector voltages but maintains its similar shape to earlier trials on the same day.

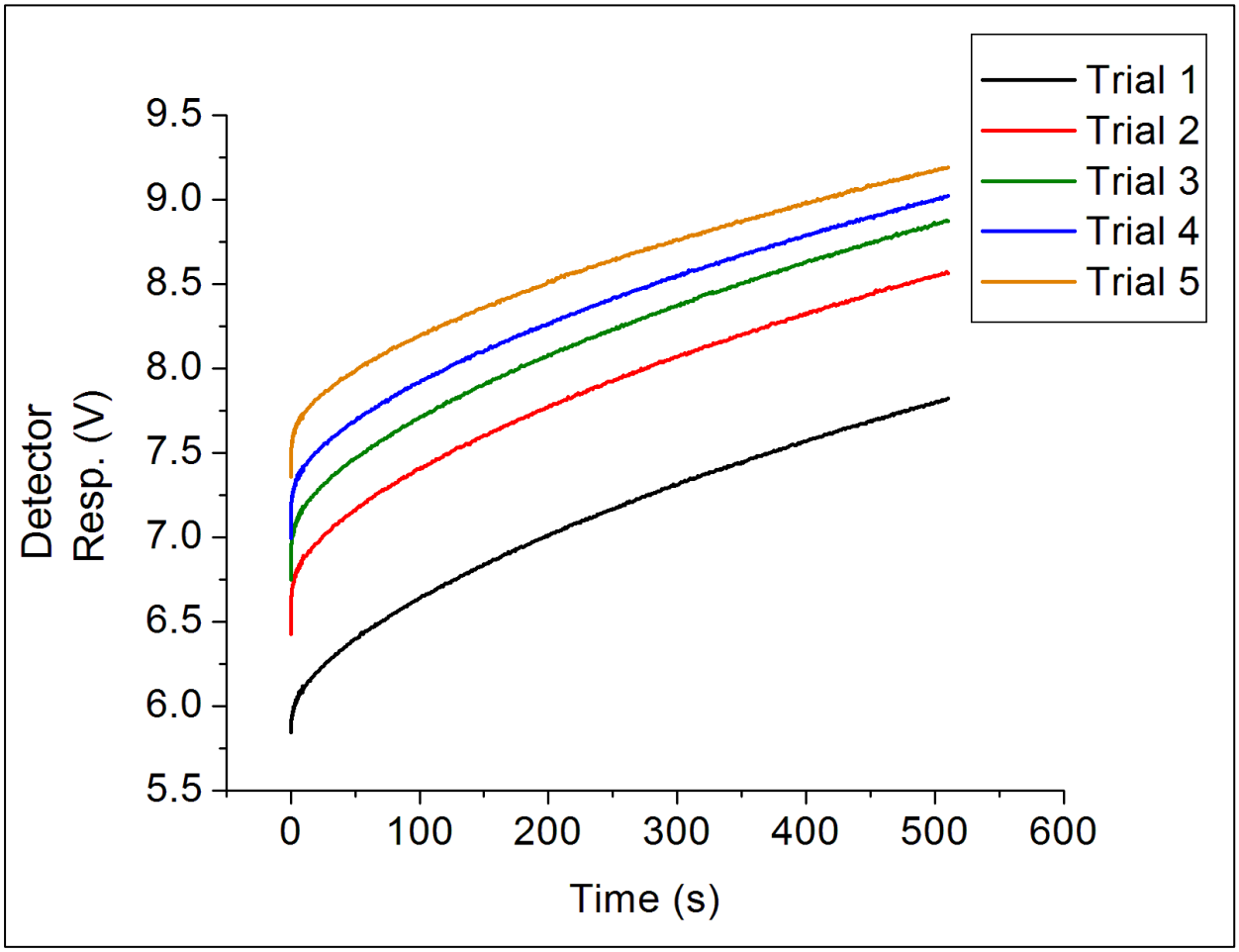

Figure 3.2.3- Stopped-flow plots of the acceptor channel for dark state adapted trials of LOV1 C83S Cy3 and LOV1 C57G C83S Cy5 mixture. Trials were performed in sequential order on the same day.

Table 3.2.2- Time constants (τ_1, τ_2) and relative amplitudes (A_1, A_2) *for FRET paired LOV1 C83S Cy3 mixed with LOV1 C57G C83S Cy 5 in dark only mixing. Curves for the acceptor channel were fit via two components.*

Trial	1	2	3	4	5	Avg. (1-5)
τ_1 (s)	13 ±1	10 ±1	10 ±1	10 ±1	10 ±1	11 ±1
τ_2 (s)	516 ±5	499 ±7	503 ±7	500 ±7	499 ±7	503 ±6
A_1	0.24 ±0.01	0.28 ±0.01	0.28 ±0.01	0.27 ±0.01	0.25 ±0.01	0.26 ±0.01
A_2	2.6 ±0.1	2.5 ±0.1	2.5 ±0.1	2.4 ±0.1	2.2 ±0.1	2.4 ±0.1

3.2c) Discussion

If left in the dark, the LOV domains of *Chlamydomonas reinhardtii* (*C.r.*) are known to favor monomers over dimers.[15] However, upon exposure to blue wavelengths of light, the domains change conformational shape to increase the amount of dimers that exist.[15] Using this knowledge, we used stopped-flow spectroscopy to see if we could monitor dimer formation by detecting and monitoring FRET between *C.r.* LOV domains.

Figure 3.2.1 gives the detector responses for the donor channel (figure 3.2.1a, top left) and acceptor channel (figure 3.2.1b, top right) for each run of LOV1 WT Cy3 mixed with LOV1 C57G C83S Cy5 in its dark state. The plots of figure 3.2.1 do in fact support that FRET can be monitored between *C.r.* LOV domains. For stopped-flow, we expected that mixing monomers in the dark state would not generate FRET. When exposed to blue light, mixed donor and acceptor samples should dimerize and FRET should be observed in the acceptor channel. Figures 3.2.1a and 3.2.1b demonstrates this previous statement. Figure 3.2.1a shows the response curves decreasing in value over time, which makes sense for photobleaching given the total data collection time and knowing that the mixing chamber is constantly exposed to 500 nm wavelength light. In the dark state, figure 3.2.1b also supports that minimal interaction between LOV monomers would not cause a significant, if any, rise in the acceptor channel's signal. The signal observed in figure 3.2.1b for each run comes from the crosstalk between the donor and acceptor channel detectors, which we calculated to be ~6% of the total signal in the acceptor channel. The plots in figure 3.2.1b also display more noise than the plots in figure 3.2.1a, which is due to the manual adjustment of the voltage for each detection channel's photomultiplier tube in order to attain an adequate sensitivity to detect signal.

We expected exposing *C.r.* LOV monomers to blue light to cause a shift in equilibrium that would favor dimers. Figure 3.2.1c gives overlaid plots of the donor and acceptor channel responses versus time after the injection of light state adapted LOV1 wild type Cy3 and LOV1 C57G C83S Cy5 into the mixing chamber. Figure 3.2.1c demonstrates the shift in equilibrium during the light state by an increase in the acceptor channel response curve. We expect that only a change in the acceptor channel's response curve is seen because a small amount of FRET is being generated. Because of the design of the stopped-flow apparatus, samples of donor and acceptor singly labeled domains had to be exposed to blue light before mixing. This means that any signal coming from the acceptor channel, assuming cross talk and direct excitation of the acceptor are being accounted for, should be from the contribution of FRET. Also, it should be mentioned that the acceptor labeled LOV1 has the active site cysteine mutated to glycine (C57G), and thus the protein should not be responsive to blue light. However, a sharp rise in signal was recorded in the acceptor channel nonetheless, suggesting that only a single LOV1 monomer has to possess a photoactive site for dimerization to occur.

Since the overarching goal of this project was to increase understanding of the dynamics of LOV-LOV interactions, it made sense to gather kinetic data from the stopped-flow plots of detector response versus time. By knowing these plots from the acceptor channel possess an exponential curvature, we can use fitting software to recover information about the formation of dimers/oligomers. Table 3.2.1 gives the recovered time constants and relative amplitudes for a series of analyzed mixtures of light adapted LOV1 wild type Cy3 and LOV1 C57G C83S Cy5 taken over two separate days of experiments. Figure 3.2.2 displays the response curves for each day's worth of trials. Since the numerical order of the trials matches the order over which the trial

measurements were taken, it is noteworthy that (excluding trial 3) the slopes of each curve would decrease in such an ordered fashion. From table 3.2.1, we see that per each day's trials, an increase in the overall time constant was observed as trials progressed.

One possibility might be caused by the method of performing the light state exposure. Due to the design of the stopped-flow mixing chamber, we performed the blue light exposure step before every trial of mixing donor and acceptor labeled samples. At the time of performing the experiments, we did not unwrap and expose the acceptor labeled sample (LOV1 C57G C83S Cy5) to blue light because it was photoinactive. With each successive light state trial performed, it is possible that we gradually increased the amount of homodimers in the donor labeled sample syringe before mixing. This increasing number of homodimers would cause a decrease in the formation rate of heterodimers over the course of the experiment, and thus lower the amount of FRET detected with each successive trial.

The recovered values and plots from table 3.2.2 and figure 3.2.3 were all collected on samples dark adapted prior to mixing LOV1 C83S Cy3 and LOV1 C57G C83S Cy5. Compared to table 3.2.1 (light adapted) values recovered from data in figure 3.2.2, the time constants in table 3.2.2 appeared more consistent in value over time but smaller in value on average. The difference in the magnitude of the time constants may be caused by free donor and acceptor dye that is noncovalently bound coming on and off the surface of proteins, which we knew may exist based on previous failed labeling attempts incorporating size exclusion chromatography separation and mass spectrometry on the LOV domains. The consistency of the time constants in table 3.2.2 versus table 3.2.1 may be attributed to the sample being in the dark state for the entire experiment set, shown in figure 3.2.3. It is still unclear how to explain plots of figure 3.2.3, which

display a rise in the acceptor channel for dark state adapted mixtures of LOV1 C83S Cy3 and LOV1 C57G C83S Cy5. Possibly for some reason, LOV1 C83S Cy3 forms dimers more readily with LOV1 C57G C83S Cy5 than LOV1 wild type forms dimers, although this appears unlikely. It is also possible that the dialysis used on each of the donor and acceptor samples was compromised, given the dialysis procedure for the experiment was performed by the experimenter for the first time and since we have shown undialyzed samples do produce fast detection responses for FRET with values less than ~10 seconds. The translation of each curve in figure 3.2.3 to a higher detector response could be simply drift in the photomultiplier tubes over time. However, it is odd that the drift would continually rise over the course of tens of minutes.

Based on the recovered time constants from the fits and knowing that only photoactive donor-labeled LOV1 was illuminated prior to mixing with the acceptor labeled LOV, we propose that two reactions are occurring to generate the values of the presented time constants. Within the mixing chamber, a signal response from the acceptor channel would be caused by donor and acceptor labeled LOV1 monomers interacting. A model consistent with our observations is the following:

$$LOV1^{*}\ Cy3 + LOV1\ Cy5 \rightleftharpoons Cy3\ LOV1^{*}\text{-}LOV1\ Cy5 \qquad \textit{Reaction 3.2.1}$$

$$LOV1^{*}\ Cy3 + LOV1^{*}\ Cy3 \rightleftharpoons Cy3\ LOV1^{*}\text{-}LOV1^{*}\ Cy3 \qquad \textit{Reaction 3.2.2}$$

where * designates the adduct state. Within the sample syringe, an increasing amount of photoactive LOV1 Cy3 is forming homodimers caused by blue light exposure with each subsequent trial. The rate of appearance of FRET would then be described by the equation below,

$$Rate = k_{forward}[LOV1^{*}\ Cy3][LOV1\ Cy5] - k_{reverse}[Cy3\ LOV1^{*}\text{-}LOV1\ Cy5] \qquad \textit{Eq. 3.2.2}$$

where $k_{forward}$ and $k_{reverse}$ represent the rate constants for the formation and dissociation of heterodimers respectively (reaction 3.2.1, above). It is logical to think that if FRET were occurring in the mixing chamber, light activated monomers forming heterodimers would contribute to the recovered time constant (τ_1) representing the faster process. A second, slower process would be represented by the second recovered time constant (τ_2), associated with light activated homodimers, which would first have to dissociate to form heterodimers that contribute to the appearance of FRET.

In summary, we applied stopped-flow spectroscopy techniques to monitor the appearance of FRET within mixture of donor and acceptor labeled LOV1 domains of *Chlamydomonas reinhardtii*. We have demonstrated a change in the FRET responses between mixed samples of LOV1 domains where only the donor labeled LOV is light adapted. Based on the results from the recoveries of two-component fits for each sample mixture, dimer formation between *C.r.* LOV domains possesses a fast (~10^1 s) and slow (~10^2-10^3 s) process. Based on our experiments, it is hypothesized that there are two reactions to form dimers, perhaps by light adapted homodimer formation where both are in their adduct states or heterodimer formation upon mixing where only the donor labeled LOV is in its adduct state.

4) Conclusions and Future Directions

From the work presented on single molecule burst measurements, we observed a change in apparent FRET efficiency for *Rhodobacter sphaeroides* (*Rsp)* samples that was greater when mixtures were exposed to continuous blue light at micromolar concentration, then incubated in the dark for several hours to reacquire the dark reversion state. This indicates that heterodimers form in the dark reversion state for *Rsp* LOV and are detected by measuring FRET. Measurements attempting to determine the K_d also showed FRET, indicating heterodimer formation in the dark reversion state, but the data used to create the K_d plot was not conclusive enough to allow for a K_d value to be found.

Single molecule burst measurements on LOV1 from *Chlamydomonas reinhardtii* (*C.r.*) showed no significant change in the apparent FRET efficiency between dark adapted, light adapted, and dark-reverted states, indicating no significant change in the ratio of monomers to dimers when the domains were in the dark or light adapted states.

Stopped-flow spectroscopy on *C.r.* LOV1 domains did show a response in the acceptor channel for sample mixtures exposed to blue light, indicating FRET between heterodimers was occurring. The recovered time constants from fitting the detector response curves indicates a slow and fast process occurring between *C.r.* LOV1 domains we attribute to the formation of heterodimers within the mixing chamber and formation of light adapted homodimers prior to mixing.

Future work requires further investigation of the LOV-LOV interactions for *C.r.*, given that phototropin from *C.r.* contains two LOV domains called LOV1 and LOV2. The interactions of LOV1-

LOV1 dimers may be different versus LOV1-LOV2 dimers, and it would be interesting to observe how the recovered time constants would change. Since we observed no significant FRET in *C.r.* sample mixtures for burst measurements, it would be logical to test whether greater amounts of FRET would be detected between LOV1-LOV2 interacting. Ideally, both donor and acceptor labeled LOV samples would be photoactive for such experiments. Due to the difficulty of successfully labeling LOV1 with Cy5 dye, we were limited in what samples we could use for single molecule and stopped flow experiments. Based on the presented data, the low concentration (pM) at which single molecule fluorescence measurements are performed may hinder heterodimer formation for LOV from both *Chlamydomonas reinhardtii* and *Rhodobacter sphaeroides*. From the data, if single molecule measurements were to be repeated with any variant of LOV, samples should be mixed at higher concentrations (e.g., 10^1 µM) before equilibration in the dark and then quickly diluted prior to taking measurements. Being able to continuously expose the samples to blue light during experiments without risk of damaging the detectors may also aid to enhance the observed change in FRET efficiency between dark and light state experiments. Both single molecule and stopped-flow measurements would benefit from such a capability, with the stopped-flow instrumentation additionally allowing for blue light exposure to be performed within the mixing chamber.

References

1. Christie, J. M. (2007). Phototropin blue-light receptors. Annual Review of Plant Biology. **58:** 21-45.

2. Kottke, T., et al. (2006). "The photochemistry of the light-, oxygen-, and voltage-sensitive domains in the algal blue light receptor phot." Biopolymers **82**(4): 373-378.

3. Swartz, T. E., et al. (2001). "The Photocycle of a Flavin-binding Domain of the Blue Light Photoreceptor Phototropin." Journal of Biological Chemistry **276**(39): 36493-36500.

4. Okajima, K. (2016). "Molecular mechanism of phototropin light signaling." Journal of Plant Research **129**(2): 149-157.

5. Christie, J. M., et al. (1998). "Arabidopsis NPH1: A Flavoprotein with the Properties of a Photoreceptor for Phototropism." Science **282**(5394): 1698-1701.

6. Conrad, K. S., et al. (2014). "Photochemistry of Flavoprotein Light Sensors." Nature chemical biology **10**(10): 801-809.

7. Briggs, W. R. and J. M. Christie (2002). "Phototropins 1 and 2: versatile plant blue-light receptors." Trends in Plant Science **7**(5): 204-210.

8. Kasahara, M., et al. (2002). "Photochemical Properties of the Flavin Mononucleotide-Binding Domains of the Phototropins from Arabidopsis, Rice, andChlamydomonas reinhardtii." Plant Physiology **129**(2): 762-773.

9. Salomon, M., et al. (2000). "Photochemical and Mutational Analysis of the FMN-Binding Domains of the Plant Blue Light Receptor, Phototropin." Biochemistry **39**(31): 9401-9410.

10. Takakado, A., et al. (2017). "Light-Induced Conformational Changes of LOV2-Kinase and the Linker Region in Arabidopsis Phototropin2." The Journal of Physical Chemistry B **121**(17): 4414-4421.

11. Christie, J. M., et al. (2002). "Phototropin LOV domains exhibit distinct roles in regulating photoreceptor function." The Plant Journal **32**(2): 205-219.

12. Harper, S. M., et al. (2003). "Structural Basis of a Phototropin Light Switch." Science **301**(5639): 1541-1544.

13. Yamamoto, A., et al. (2009). "Light Signal Transduction Pathway from Flavin Chromophore to the Jα Helix of Arabidopsis Phototropin1." Biophysical Journal **96**(7): 2771-2778.

14. Salomon, M., et al. (2004). "Dimerization of the plant photoreceptor phototropin is probably mediated by the LOV1 domain." FEBS Letters **572**(1-3): 8-10.

15. Kutta, R. J., et al. (2008). "Blue-Light Induced Interaction of LOV Domains from Chlamydomonas reinhardtii." ChemBioChem **9**(12): 1931-1938.

16. Katsura, H., et al. (2009). "Oligomeric structure of LOV domains in Arabidopsis phototropin." FEBS Letters **583**(3): 526-530.

17. Nakasako, M., et al. (2004). "Light-Induced Structural Changes of LOV Domain-Containing Polypeptides from Arabidopsis Phototropin 1 and 2 Studied by Small-Angle X-ray Scattering." Biochemistry **43**(47): 14881-14890.

18. Matsuoka, D. and S. Tokutomi (2005). "Blue light-regulated molecular switch of Ser/Thr kinase in phototropin." Proceedings of the National Academy of Sciences of the United States of America **102**(37): 13337-13342.

19. Stryer, L. and R. P. Haugland (1967). "Energy transfer: a spectroscopic ruler." Proceedings of the National Academy of Sciences **58**(2): 719-726.

20. Van Der Meer, B. W., et al. (1994). Resonance Energy Transfer: Theory and Data, Wiley.

21. Ha, T. (2001). "Single-Molecule Fluorescence Resonance Energy Transfer." Methods (San Diego, CA, United States) **25**(1): 78-86.

22. Sisamakis, E., et al. (2010). "Accurate Single-Molecule FRET Studies Using Multiparameter Fluorescence Detection." Methods in Enzymology **475**: 455-514.

23. Margittai, M., et al. (2003). "Single-molecule fluorescence resonance energy transfer reveals a dynamic equilibrium between closed and open conformations of syntaxin 1." Proceedings of the National Academy of Sciences **100**(26): 15516-15521.

24. Deniz, A. A., et al. (1999). "Single-pair fluorescence resonance energy transfer on freely diffusing molecules: Observation of Förster distance dependence and subpopulations." Proceedings of the National Academy of Sciences **96**(7): 3670-3675.

25. DeVore, M. S., et al. (2012). "Classic Maximum Entropy Recovery of the Average Joint Distribution of Apparent FRET Efficiency and Fluorescence Photons for Single-Molecule Burst Measurements." The Journal of Physical Chemistry B **116**(13): 4006-4015.

26. Conrad, K. S., et al. (2013). "Light-Induced Subunit Dissociation by a Light–Oxygen–Voltage Domain Photoreceptor from Rhodobacter sphaeroides." Biochemistry **52**(2): 378-391.

27. Sakamoto, K. and W. R. Briggs (2002). "Cellular and Subcellular Localization of Phototropin 1." The Plant Cell **14**(8): 1723-1735.

28. Wada, M., et al. (2007). Light Sensing in Plants, Springer Japan.

29. Christie, J. M. (2007). Phototropins and Other LOV-containing Proteins. Annual Plant Reviews Volume 30: Light and Plant Development, Blackwell Publishing Ltd**:** 49-78.

30. Chance, B. (2004). "The Stopped-flow Method and Chemical Intermediates in Enzyme Reactions - A Personal Essay." Photosynth Res **80**(1-3): 387-400.

31. Engel, T., et al. (2008). Physical Chemistry for the Life Sciences, Pearson Prentice Hall.

32. Gakamsky, D. M., et al. (2007). "Kinetic evidence for a ligand-binding-induced conformational transition in the T cell receptor." Proceedings of the National Academy of Sciences of the United States of America **104**(42): 16639-16644.

33. Tims, H. S. and J. Widom (2007). "Stopped-flow fluorescence resonance energy transfer for analysis of nucleosome dynamics." Methods (San Diego, CA, United States) **41**(3): 296-303.

34. Fedorov, R., et al. (2003). "Crystal Structures and Molecular Mechanism of a Light-Induced Signaling Switch: The Phot-LOV1 Domain from Chlamydomonas reinhardtii." Biophysical Journal **84**(4): 2474-2482.